2010

Luminal calcium regulates membrane fusion in the early secretory pathway

Marvin Bentley
The University of Montana

LUMINAL CALCIUM REGULATES MEMBRANE TRAFFICKING IN THE EARLY SECRETORY PATHWAY

By

MARVIN DOMINIC JAMES BENTLEY

B.A., Ouachita Baptist University, AR, 2004

Dissertation

presented in partial fulfillment of the requirements
for the degree of

Doctor of Philosophy
Integrative Microbiology and Biochemistry, Cellular and Molecular Biology

The University of Montana
Missoula, MT

December 2010

Approved by:

Perry Brown, Associate Provost for Graduate Education
Graduate School

Jesse Hay, Chair
Division of Biological Sciences

Scott Wetzel
Division of Biological Sciences

Mark Grimes
Division of Biological Sciences

Scott Samuels
Division of Biological Sciences

Darrell Jackson
Department of Biomedical and Pharmaceutical Sciences

Bentley, Marvin, Ph.D., Fall 2010 Cell Biology

Luminal calcium is a regulator in the early secretory pathway

Chairperson: Jesse Hay

Calcium is an important regulatory ion which acts as a trigger or is required at a basal level for many membrane fusion events. The role of calcium, and in particular luminal calcium, in regulating fusion in the early secretory pathway has not been thoroughly investigated. Here, I show that calcium has an inhibitory effect on homotypic coat protein complex (COPII) vesicle fusion. In particular, chelation of luminal calcium as well as fast chelation of extra luminal calcium, result in a significant increase of COPII vesicle fusion. Specific inhibition of Sarco/endoplasmic reticulum calcium ATPases using cyclopiazonic acid in the presence of calcium free medium results in low luminal calcium while maintaining normal calcium concentration in the cytosol. This luminal calcium depletion results in a dramatic expansion of the endoplasmic reticulum to Golgi intermediate compartment (ERGIC) in the periphery of the cell visualized using the markers rbet1 and p24. Depletion of luminal calcium also results in major kinetic defects of VSV-G transport to the Golgi, as well as reconstitution of the Golgi after it has been dispersed using brefeldin A. These results suggest that luminal calcium regulates fusogenicity, structure, and function of COPII derived membranes in transport. However, bulk soluble cargo is not affected by luminal calcium depletion. This suggests that luminal calcium may act at the level of membrane protein sorting in the ERGIC. Possible mechanisms by which luminal calcium exerts these novel roles are discussed herein and include prolonged retention of the outer COPII shell Sec13/Sec31 with Apoptosis Linked Gene-2 (ALG-2) being a likely candidate as the calcium sensor on the outside of the vesicle.

Dedicated to:

Bryan DeBusk

Amanda Dawsey & Tod Bachman

Fabian Bentley

Acknowledgements

I thank the following people for their help and support in accomplishing this task:

Jesse Hay: For supporting me as my advisor throughout the time it took me to complete my research and write this dissertation. Thank you for giving me a chance to become a scientist.

Scott Wetzel: For letting me spend many pleasant hours in your office and for teaching me everything that I know about microscopy.

My committee members Darrell Jackson, Mark Grimes, and Scott Samuels, who have generously given their time and expertise to better my work and my abilities as a scientist. I thank them for their contribution and their support.

The members of the Hay laboratory: Nandhakumar Thayanidhi, Ting Wang, and Deb Nycz for providing friendly support and for contributing experiments to my thesis.

The office staff: Sherrie Wright, Jill Burke, Janean Clark, Kate Stewart and Jen Geist.

Bryan DeBusk: For being a wonderful friend and my first and greatest science teacher. Thank you for convincing me to go to graduate school.

Amanda Dawsey and Tod Bachman: My family away from home.

Meg Trahey: For being my favourite graduate school teacher, for being an encouraging friend in the laboratory, and of course for spending endless hours helping me edit this dissertation.

Jared Helm: For reviewing the dissertation, but mostly for your friendship.

Hayley Blackburn: I will always wait the extra five (!) minutes it takes for you to get there.

Eli Loomis: My first friend in graduate school. I will always remember training seminar.

Denise Birkholz: For career advice and for being my friend.

My friends of Red Rum: Joran Elias, Steve Patterson, Sarah Tarka, Alex Baer, Rebecca Shern, Weston Wade, Tri Pham, and Audrey Elias.

Fabian Bentley: The best brother anybody could ever hope for.

My parents: Thank you for always being supportive, including letting me go at a young age to pursue my academic goals. Without your encouragement and help I would have never made it this far.

Table of Contents

INTRODUCTION AND BACKGROUND 1
I The secretory pathway is an essential cellular system 1
II ER to Golgi transport is the rate limiting step of cargo secretion 4
Export from the endoplasmic reticulum 4
Cargo adaptors on COPII vesicles 7
Rab GTPases and tethers 8
SNAREs in the secretory pathway 10
Regulation of SNARE activity 11
Cargo in the secretory pathway 11
ERGIC to Golgi transport 13
III Endoplasmic reticulum stress and ATF-6 14
IV Calcium in the secretory pathway 16
Calcium is a regulator of several membrane fusion events 16
The endoplasmic reticulum is the primary cellular storage compartment for calcium 18
Calcium chelators 19

MATERIALS AND METHODS 26
Depletion of luminal calcium 26
Immunofluorescence 26
Quantification of Images 28
Brefeldin A recovery assay 29
ATF-6 detection 30
VSV-G trimer precipitation 30
Antibodies 31
Luminal calcium measurements 32
Heterotrimerization fusion assay 33

RESULTS 35
Fast chelation of calcium during *in vitro* COPII vesicle fusion reveals a role for luminal calcium 35
Depletion of luminal calcium in intact cells results in an enlarged ER to Golgi intermediate compartment 37
ERES do not change their size in calcium depleted cells 42
VSV-G trafficking can be measured using intact cells and fluorescence microscopy 43
VSV-G trafficking in intact cells is impaired at a post folding stage by luminal calcium depletion 46
Golgi reformation after brefeldin A treatment is impaired in calcium depleted cells. 49
Bulk soluble cargo in HeLa cells is not affected by luminal calcium depletion 50

Luminal calcium depletion does not result in ATF-6 unfolded protein response activation 51

DISCUSSION 82
Major contributions of this thesis to the field 82
Luminal calcium suppresses COPII vesicle fusion *in vitro* 83
Luminal calcium regulates the distribution of intermediate compartment elements 86
Luminal calcium is required for optimal ER to Golgi transport of membrane proteins 87

REFERENCES 91

List of Figures

1. The secretory pathway 21
2. Endoplasmic reticulum to Golgi transport leads through the ER to the Golgi intermediate compartment 22
3. Schematic of COPII vesicle formation 23
4. Calcium puffs can elevate local calcium concentrations 24
5. Chemical structures of EGTA and BAPTA 25
6. BAPTA enhances COPII vesicle fusion *in vitro* 53
7. Membrane permeant EGTA and BAPTA enhance homotypic COPII vesicle fusion 54
8. Additional calcium increases the amount of BAPTA required for stimulation of homotypic COPII vesicle fusion 55
9. CPA treatment results in decreased luminal calcium 56
10. Cytosolic calcium returns to normal levels after 15 minutes of CPA treatment 57
11. Calcium depletion and 15°C treatment results in dramatic enlargement of ERGIC structures 58
12. Average rbet1 object size increases during luminal calcium depletion 59
13. Average rbet1 object size increases with different calcium depleting drugs and is not dependent on new rbet1 synthesis 60
14. Luminal calcium and 15°C treatment result in distinct changes in rbet1 distribution 61
15. Total rbet1 immunofluorescence increases upon depletion of luminal calcium as well as incubation at 15°C 62
16. Total rbet1 expression does not change significantly upon depletion of luminal calcium or incubation at 15°C 63
17. Total GM130 immunofluorescence remains constant during depletion of luminal calcium as well as incubation at 15°C 64
18. Luminal calcium depletion results in the enlargement of p24 positive ERGIC structures 65
19. Luminal calcium depletion results in the production of p24 positive ERGIC structures of different sizes 66
20. Sec16 ERES staining remains unchanged following luminal calcium depletion 67
21. Sec16 peripheral object abundance remains unchanged in cells depleted of luminal calcium 68
22. Syntaxin 5 is knocked down more than 90% in NRK cells 70
23. VSV-G-GFP trafficking impairment due to Syntaxin 5 knockdown is measurable using the transport index ratio 71
24. Depletion of luminal calcium decreases ER to Golgi transport of VSV-G-GFP 72
25. VSV-G trimerizes maximally in three minutes 73
26. VSV-G-GFP trimers are transport more slowly to the Golgi apparatus following luminal calcium depletion 74

27. Golgi recovery after brefeldin A washout is impaired in cells depleted of luminal calcium 75
28. Graphical representation of the conditional aggregation domain 76
29. Calcium depletion in HeLa cells results in an increase of large peripheral structures 77
30. Bulk cargo transport is not affected by the depletion of luminal calcium 78
31. Cargo de-aggregation occurs at a rapid rate for control and CPA treated cells 79
32. ATF-6 is not activated by typical conditions for luminal calcium depletion 80
33. A model for cargo sorting in the ERGIC 90

List of Tables

1. Co-localization of large peripheral objects 69

Introduction and Background

I -- The secretory pathway is an essential cellular system

The secretory pathway is an essential organizational system of eukaryotic cells. Up to one third of all cellular proteins require transit through this pathway to reach their ultimate destinations (Levine et al., 2005). These destinations include lysosomes, secretory granules, endosomes, synaptic vesicles, the plasma membrane, and the extracellular space. The primary intracellular compartments involved in transport are the endoplasmic reticulum (ER) and the Golgi apparatus (Figure 1).

The ER is a membranous network consisting of interconnected tubules and cisternae, which takes up more than half of the total cellular membrane. The ER is distributed around the nucleus and from there it extends throughout the cytoplasm of the cell. The ER functions as a site for lipid synthesis, as well as well as protein folding. The ER also acts as the primary calcium storage compartment for the cell.

The ER surface is classified as either "rough" or "smooth." The rough ER is characterized by the presence of ribosomes, which gives it a rough appearance in EM micrographs and is an area of active protein biosynthesis. Proteins destined for the ER have a signal sequence at their N-terminus. While these signal sequences exhibit great variation in amino acid sequence, each signal sequence contains a minimum of eight non-polar amino acids at the center. The signal sequence is recognized by the signal-recognition particle (SRP), a hetero-hexameric protein attached to a small RNA molecule. As soon as the nascent amino acid chain starts exiting the ribosome, SRP

recognizes the hydrophobic signal sequence and binds to the ribosome. This interaction arrests translation. While translation is arrested the ribosome attaches to the SRP receptor which is located in the ER membrane. The SRP receptor then mediates the hand-off of the nascent polypeptide ribosome to the translocon, after which translation resumes.

Soluble proteins are simply transported through the translocator in one piece. However, type I single pass transmembrane proteins on the other hand have an additional hydrophobic stop transfer signal. Once the stop transfer signal is reached the translocator releases the polypeptide and further translation is completed in the cytosol, resulting in a single pass membrane anchored protein. Proteins with several transmembrane domains also contain internal start transfer signals, which recruit a translocator (Alberts et al., 2008).

After translocation, proteins are folded in the ER. There are several ER resident chaperones that aid in protein folding. Protein disulfide isomerase (PDI) aids in the formation of disulfide bonds between cysteines (Bassuk and Berg, 1989). Proteins of the Hsp90 family help a variety of proteins in their folding and maturation (Taipale et al., 2010).

After proteins complete folding, they are glycosylated in the ER. During protein glycosylation a large sugar chain containing N-acetylglucosamine, mannose, and glucose is transferred to the target side chain, an asparagine residue. The reaction is catalyzed by the ER membrane oligosaccharyl transferase. While this is a transmembrane protein, the active domain is located on the luminal side of the ER membrane. Glycosylation in the ER allows quality control of the folding state of the protein. Improperly folded proteins

have single glucose molecules added to their N-linked oligosaccharides by glucosyl transferase. These single glucose molecules are then recognized by sugar binding (lectin) chaperones, such as calnexin. Calnexin is attached to the ER membrane and retains any unfolded proteins in the ER. This allows the protein to properly fold and have the glucose removed, at which point the protein can leave the ER.

Figure 1 shows a diagram of the secretory pathway (Alberts et al., 2008). After proteins are properly folded, glycosylated, and assembled in the ER, they are packaged into transport vesicles that bud from the ER. The bud is formed by members of the coat protein II (COPII) group. These coat proteins define the identity of the vesicle as it leaves the ER and is destined for the ER to Golgi intermediate compartment (ERGIC). Mature vesicles fuse with each other or with the ERGIC. In the ERGIC cargo is sorted. Coat protein I (COPI) vesicles bud off from here to retrieve wayward ER proteins and return them to the ER. After the cargo is sorted here, the ERGIC attaches to microtubules and is transported to the Golgi apparatus with the help of dynein motor proteins. As the ERGIC approaches the Golgi it receives COPI vesicles that are derived from the *cis*-Golgi. These slowly change the identity of the ERGIC compartment into a cisterna of the *cis*-Golgi. This membraneous compartment then flattens out and slowly travels through the Golgi apparatus (Figure 2). Inside the Golgi apparatus proteins are further modified. In the *cis*-Golgi covalently attached sugars that were attached to the protein in the ER are further modified. Example enzymes that mediate such sugar processing are Mannosidase I and Mannosidase II, the latter removing mannose groups from oligosaccharides, rendering the sugar insensitive to Endo-H cleavage. After proper processing, proteins are released from the *trans*-Golgi.

From the *trans*-Golgi proteins are packaged into vesicles and transported to their final destination. This can lead through late endosomes to lysosomes. The main pathway for constitutive secretion leads directly from the *trans*-Golgi network to the plasma membrane. Neurotransmitter proteins are packaged into synaptic vesicles that bud from recycling endosomes before they head to the plasma membrane, where they can fuse and release their cargo into the extracellular space (Alberts et al., 2008).

II – ER to Golgi transport is the rate limiting step of cargo secretion

Export from the Endoplasmic Reticulum

The first step in ER to Golgi transport is the budding of small vesicles that are generated at ER Exit Sites (ERES) (Kirk and Ward, 2007). ERES are specialized regions of the ER that are ribosome free, but have high concentrations of the coat protein complex COPII (Hughes and Stephens, 2008). These regions function to concentrate cargo and to generate COPII vesicle buds. COPII is a multi-protein complex that is involved in the accumulation of cargo at the ERES as well as the deformation of the ER membrane and the subsequent budding of the vesicle (Bielli et al., 2005; Lee et al., 2005). ERES have been found in all eukaryotic cells including yeast (Wooding and Pelham, 1998), protozoan parasites (He et al., 2001), and plants (daSilva et al., 2004).

The primary regulating protein involved in vesicle formation is the COPII small GTPase Sar1. Sar1 is a soluble protein and is recruited to the ERES membrane by its Guanine Nucleotide Exchange factor (GEF) Sec12 (Nakano et al., 1988). Sec12 initiates the exchange of GDP for GTP that results in activated Sar1. Sar1 then starts initial

deformation of the ER membrane, by changing its structure and inserting its N-terminal amphipathic helix into the membrane (Bielli et al., 2005). After attaching to the membrane, Sar1 recruits the inner shell of the COPII coat to the ERES. This shell is composed of Sec23/Sec24 (Barlowe et al., 1994). The recruitment is mediated by direct interaction of Sar1 and Sec23 (Figure 3) (Budnik and Stephens, 2009). Sec23 also acts as the Sar1 GTPase Activating Protein (GAP), while Sec24 is involved in cargo binding (Aridor et al., 1998). The outer COPII shell, consisting of the heterodimer Sec13/Sec31, is recruited after cargo binds to Sec23/Sec24 and formation of the pre-budding complex (Fath et al., 2007). This final layer of the COPII coat consists of hetero-tetramers which are made up of two Sec13 and two Sec31 subunits that self assemble into a cage like structure. This cage defines the structure of the vesicle that then forms a bud at the ERES. Completion of this assembly results in the budding of a coated vesicle that is loaded with cargo and prepared to move away from the ER. Sar1 hydrolyzes its GTP before membrane fission can be completed (Bielli et al., 2005). The process of assembling COPII coated vesicles can be reconstructed *in vitro* using just liposomes and the five above mentioned proteins (Sar1, Sec23, Sec24, Sec13, and Sec31) (Matsuoka et al., 1998).

The mechanism of vesicle formation and budding from the ERES has been extensively studied (Budnik and Stephens, 2009). Immunofluorescence microscopy visualizes ERES as punctate structures found throughout the periphery of the cell. However, ERES cannot be resolved from the ERGIC by basic light microscopy. This is because the ERGIC assembles very near ERES. Electron microscopy or advanced light

microscopy techniques, such as Stimulated Emission Depletion are required for sufficient resolution.

In vivo, the budding of COPII vesicles is temperature-dependent. At 10°C, membrane fission is thermodynamically inhibited (Mezzacasa and Helenius, 2002). Thus, this can be used experimentally as an artificial block of ER cargo release in the laboratory. A temperature shift back to a permissive temperature allows budding to resume.

In addition to COPII and cargo proteins, ERES also contain the structural protein Sec16. Sec16 is a 240 kD peripheral membrane protein that is found on the ER membranes where it plays a central role in maintaining the organization of ERES (Budnik and Stephens, 2009; Espenshade et al., 1995). A function impairing mutation of Sec16 results in a general breakdown in ERES organization (Connerly et al., 2005; Rossanese et al., 1999). Sec16 was originally discovered and studied in yeast (Novick et al., 1980), but is also found in mammalian cells (Watson et al., 2006) and is likely conserved in all eukaryotic cells.

Sec16 is localized to ERES and overexpression as well as knockdown of the protein result in disruption of ER to Golgi transport (Bhattacharyya and Glick, 2007; Iinuma et al., 2007; Watson et al., 2006). In addition to interacting with Sec23/Sec24 and Sec13/Sec31, Sec16 also stabilizes the active vesicle budding complex by interacting with Sar1 as well as the structural coat proteins (Budnik and Stephens, 2009; Supek et al., 2002). Electron microscopy has revealed that the distribution of Sec16 is limited to the ER membrane and that the protein does not get loaded onto COPII vesicles. At the ERES, Sec16 immunogold labeling does not overlap with COPII labeling, showing a

clear spatial separation between the two sets of proteins. This shows that the ERES is clearly divided in cargo assembly areas, which contain Sec16, and budding sites that generate fully loaded vesicles (Hughes et al., 2009).

Cargo adaptors on COPII vesicles

In addition to the structural proteins outlined above, COPII vesicles are loaded with a plethora of regulatory and cargo proteins. Cargo adaptor proteins play an important role in enriching COPII vesicles with the correct proteins. ER resident proteins need to be excluded from the vesicle while cargo molecules are concentrated. Cells lacking cargo receptors display selective cargo trafficking defects (Strating and Martens, 2009; Zhang et al., 2009). This shows that cargo adaptor proteins are specific for certain cargo, rather than facilitating bulk export. Additionally, these proteins have been observed in the ER, the intermediate compartment, as well as the Golgi, indicating that they travel throughout the early secretory pathway (Dancourt and Barlowe, 2010).

The prototypical cargo adaptor protein is ERGIC-53, a 58 kD protein that has become one of the primary identifiers of the ERGIC. ERGIC-53 has binding sites on the C-terminus that interact with Sec23/Sec24, targeting it directly to the inner shell of the COPII vesicle coat. The luminal domain of ERGIC-53 interacts with the glycosylated coagulation factors V and VIII, which do not traffic efficiently when ERGIC-53 is dysfunctional (Moussalli et al., 1999). Deficiency in these coagulation factors predisposes individuals towards haemophilia. Interestingly, deficiencies in another protein, MCFD2, result in phenotypes indistinguishable from dysfunctional ERGIC-53 (Zhang et al., 2005). MCFD2 is assembled in a calcium dependent manner into a

complex with ERGIC-53. MCFD2 and ERGIC-53 co-localize based on immunofluorescence data (Nyfeler et al., 2006). MCFD2 contains two calcium binding EF-hand motifs. If either of these is mutated to prevent calcium binding, MCFD2 cannot fold correctly and is prevented from interacting with ERGIC-53 (Guy et al., 2008; Zhang et al., 2006). This means that calcium plays an important role for cargo sorting in the lumen of the ER and in particular in ERES.

Another cargo adaptor protein family prominently active in the early secretory pathway is the p24 receptor family. Originally p24 was identified as a membrane protein that is enriched on COPII and COPI vesicles (Schimmoller et al., 1995; Stamnes et al., 1995). p24 proteins are type I transmembrane proteins of ~24 kD molecular mass. The protein has three primary structural elements: An N-terminal luminal domain, an alpha-helical transmembrane domain, and a cytoplasmic C-terminal domain that interacts with COPII (Dominguez et al., 1998). Yeast strains lacking the p24 family members Emp24 or Erv25 show trafficking defects (Belden and Barlowe, 1996; Schimmoller et al., 1995). As an example, in yeast cells lacking p24, the Golgi arrival of Gas1p and secretory invertase was measured and is significantly retarded (Muniz et al., 2000). While p24 acts as a cargo adaptor, it may have further functions, such as quality control, vesicle biogenesis, or as a structural protein in ER to Golgi transport (Aguilera-Romero et al., 2008).

Rab GTPases and Tethers

Vesicles that are ready to attach to and fuse with their target membranes require activated Rab GTPases. Rab GTPases play a key role in specificity and are expressed in

all cells, with over 60 of them identified in mammals (Grosshans et al., 2006). Rabs cycle between a cytosolic state and a membrane-bound state. In the cytosolic state, the Rab GTPase is attached to a guanine nucleotide dissociation inhibitor (GDI). With the help of a GDI displacement factor (GDF), the protein is recruited to the membrane (Dirac-Svejstrup et al., 1997). The membrane association of the Rab GTPases is mediated by a prenyl group, which is masked by the GDI (Grosshans et al., 2006). Membrane association of the Rab is correlated with the activation by a specific guanine nucleotide exchange factor (GEF) that mediates the exchange of GDP for GTP (Soldati et al., 1994; Ullrich et al., 1994). The GTP bound, activated Rab GTPase then acts on downstream effectors. Between the ER and the Golgi apparatus, Rab1 is the active Rab GTPase.

An important group of downstream Rab effectors are membrane-tethering proteins. Tethers are divided into two categories: Long rope-like proteins or multi-subunit protein complexes. These proteins make initial contact between the transport vesicle and the target compartment. The coiled coil protein p115 acts as a tether between the ER and the Golgi apparatus and is a Rab1 effector. p115 resides in the cytosol until activated Rab1 and soluble N-ethlymaleimide sensitive factor attachment protein receptors (SNAREs) recruit the tether to COPII vesicles (Bentley et al., 2006; Cai et al., 2007a). Active p115 is required for *in vitro* COPII vesicle fusion to complete (Bentley et al., 2006).

Rabs and tethers are required for membrane fusion throughout the secretory pathway. Together they act as the first structural bridge between two membranes. After

Rabs and tethers establish this first contact, other fusion machinery can engage and mediate membrane mixing.

SNAREs in the secretory pathway

As vesicles move away from the ER they need to fuse with other membranes in the secretory pathway to join their intended cargo compartment. The primary regulators of membrane fusion are soluble *N*-ethylmaleimide-sensitive factor attachment protein receptors (SNAREs). SNAREs act in the final stage of vesicular fusion, the mixing of the two membranes (Weber et al., 1998). SNAREs are classified as either v-SNAREs or t-SNAREs. v-SNAREs are associated with the vesicle, t-SNARES are located at the target membrane for the vesicle (Hong, 2005). In general, v-SNAREs are tail anchored SNARE proteins with a single SNARE motif, whereas t-SNAREs contribute three SNARE motifs to each SNARE bundle (Fukuda et al., 2000; Hong, 2005). SNAREs can be classified by their SNARE-motif. Each such motif contains either a glutamine (Q) or an arginine (R) amino acid in the center. For every four SNARE motifs that generate a bundle, there are three Q-SNAREs and one R-SNARE. After v- and t-SNAREs engage, they form a *trans*-SNARE complex, a highly organized four-helix bundle. The energy released in the formation in this bundle drives the mixing of the two opposing membranes into a fusion stalk. This eventually progresses into the presence of all SNARE proteins within a single membrane, which is the final product of membrane fusion. The four helix SNARE bundle remains arranged in a tightly bound tetramer, which does not easily dissociate and is referred to as a *cis*-SNARE complex. The best-studied exocytic synaptic vesicle SNARE complex consists of the SNARE motifs from Syntaxin1,

VAMP2, and two SNARE motifs from SNAP25 (Sutton et al., 1998). After membrane fusion, the *cis*-SNARE complex needs to be broken up, which happens in an ATP-dependent manner. This allows for the recycling of the SNARE proteins, returning functionality to the individual complex subunits.

The active SNAREs involved in mammalian COPII vesicle fusion are rbet1, membrin, Sec22, and Syntaxin5 (Dascher et al., 1994; Hay et al., 1996; Hay et al., 1998; Tang et al., 1998).

Regulation of SNARE activity

While SNARE activity is highly specific, it is also highly regulated. N-ethylmaleimide sensitive factor (NSF) and alpha-SNAP are the two primary proteins that regulate the recycling of SNAREs. An assembled *cis*-SNARE complex interacts with three molecules of alpha-SNAP and an NSF hexamer (Furst et al., 2003). NSF contains two ATPase domains that are required to have bound ATP in order for NSF to interact with alpha-SNAP (Hong, 2005). Alpha-SNAP has a region containing nine alpha helices, which form a sheet that interacts with the surfaces of the SNARE complex (Marz et al., 2003). ATP hydrolysis by NSF allows NSF/alpha-SNAP to break up SNARE complexes and releases individual fusogenic SNAREs. Accordingly, NSF and active alpha-SNAP is required for functioning ER to Golgi transport and all other transport steps (Peter et al., 1998).

Cargo in the secretory pathway

In addition to COPII components, adaptor proteins, and vesicle machinery, ERES-derived vesicles contain cargo. Several model cargo proteins have been studied, including the large molecule procollagen (Mironov et al., 2003), the soluble Semliki Forest virus capsid protein Cp (Thor et al., 2009) and, maybe most notably, the membrane protein Vesicular Stomatitis Virus Glycoprotein (VSV-G). Further, artificial cargo systems have been devised (Rivera et al., 2000; Wieland et al., 1987).

There are two separate types of ER to Golgi cargo: Bulk flow and specifically sorted cargo. Bulk flow includes soluble proteins that are not actively sorted. These are present in the ER and are not actively loaded onto COPII vesicles, but are present on the inside of the vesicle when it buds off. A typical laboratory example of bulk flow is secreted GFP (Rivera et al., 2000). Much more controlled is the transport of specifically sorted cargo like VSV-G or coagulation factor V. This type of cargo is actively sorted throughout the secretory pathway. In order for this cargo to be enriched in COPII vesicles it needs to interact with subunits of the coat or adaptor proteins.

VSV-G in particular is a membrane bound protein that has been used extensively as a model cargo. Vesicular Stomatitis Virus (VSV) is a negative sense RNA virus in the Rhabdovirus family that primarily infects cattle. VSV-G mediates the entry of the enveloped virion into the cell by receptor-mediated endocytosis (Wagner and Hewlett, 2004). Assembled VSV viral cages bud from the plasma membrane, converting the plasma membrane into the viral envelope (Strauss and Strauss, 2008). In order for VSV-G to be incorporated into the viral membrane it needs to be trafficked to the plasma membrane during viral replication. The virus uses the secretory pathway for this process, moving the molecule from the ER through the Golgi to the plasma membrane.

In the laboratory, a temperature-sensitive variant of VSV-G (ts045) is an attractive molecule because its budding from the ER can be tightly regulated (Bergmann, 1989). VSV-G needs to assemble into homotrimers in order to be released from the ER (Kreis and Lodish, 1986). At 40°C the ts045 VSV-G mutant is reversibly misfolded and cannot assemble into trimers (de Silva et al., 1993; de Silva et al., 1990). When the temperature is lowered below 40°C, trimers can then form, allowing VSV-G export from the ER and trafficking towards the Golgi. After releasing VSV-G from the ER, a temperature shift back up to 40°C does not further affect downstream trafficking (Mezzacasa and Helenius, 2002). This means that VSV-G is not required to be in trimers once it is packaged; in fact, subunits can be exchanged inside vesicle membranes while transport proceeds through the secretory pathway.

ERGIC to Golgi transport

After vesicle budding, the cargo is eventually localized to the ER-Golgi intermediate compartment (ERGIC). *In vitro* experiments with COPII vesicles have shown that they can fuse homotypically to form a *de novo* intermediate compartment (Xu and Hay, 2004). Fusion of these vesicles requires the four ER to Golgi soluble SNAREs: Syntaxin 5, membrin, rbet1, and Sec22. The study by Xu and Hay in 2004 showed that nascent COPII vesicles contain all of the machinery necessary for vesicle fusion such as SNARES and the tethering proteins p115 and TRAPP. Fusion of these vesicles requires the four ER to Golgi SNAREs Syntaxin 5, membrin, rbet1, and Sec22. All of these are present in the ERGIC and as well as the ER and the Golgi (Chao et al., 1999; Emery et al., 2000).

An important function of the ERGIC is protein sorting. This retrieval is mediated by COPI coated vesicles. Inhibiting COPI activity results in a trafficking delay of anterograde cargo, most likely caused by a failure to sort cargo in the ERGIC, which prevents the maturation of the intermediate compartment (Pepperkok et al., 1993). Another sorting mechanism is mediated by the drop in calcium at the ERGIC. As discussed above, ERGIC-53 requires calcium to bind its cargo. Calcium measurements of the secretory pathway have shown that the ERGIC has no discernable calcium (Pezzati et al., 1997), which allows ERGIC-53 to release its cargo protein as the compartment matures and loses its calcium (Appenzeller-Herzog and Hauri, 2006).

The distance from the ERGIC, which is formed close to ERES, to the *cis*-Golgi is tens of μm. In order to bridge this gap, the intermediate compartment is actively transported through the cell. The motor responsible for this transport is dynein, which binds to the dynactin complex. Disrupting this complex prevents VSV-G from trafficking to the Golgi and arrests it in the intermediate compartment (Presley et al., 1997).

As the ERGIC arrives at the Golgi, it receives COPI vesicles from the *cis*-Golgi (Alberts et al., 2008). These contain Golgi proteins and help the ERGIC take on the proteomic characteristic of the Golgi. The ERGIC eventually flattens out and becomes a Golgi cisterna.

III – Endoplasmic reticulum stress and ATF-6

Protein folding is an essential process for all life. Quality control mechanisms allow only properly folded proteins to exit the ER and travel through the secretory

pathway. Misfolded proteins are retained in the ER in order to allow chaperone proteins to facilitate refolding. Permanently misfolded proteins are sent to the ER-associated degradation pathway or degraded through autophagy (Malhotra and Kaufman, 2007).

Accumulation of a large amount of misfolded proteins in the ER presents a threat to cell viability. Because the hydrophobic effect is the driving force behind protein folding, improperly folded proteins usually have large hydrophobic patches exposed. This can result in the accumulation of large aggregates in the ER, disrupting proper ER function. In these conditions, folding chaperones are sequestered by proteins and unavailable to fold nascent polypeptide chains. Examples of ER chaperone proteins are Bip, calnexin, and GRP 94 (Argon and Simen, 1999; Gething, 1999; Ruddock and Molinari, 2006). To prevent the buildup of a large amount of misfolded protein in the ER, stressed conditions in the ER trigger the unfolded protein response.

The gatekeeper protein that regulates the cellular response to ER stress is Bip. When Bip recognizes ER stress, it activates three signaling pathways. These are inositol requiring kinase 1 (IRE1) (Sidrauski and Walter, 1997), protein kinase-like ER kinase (PERK) (Harding et al., 2000), and activating transcription factor 6 (ATF-6) (Sidrauski and Walter, 1997; Yoshida et al., 2000). Under non-stressed conditions, Bip binds to each of these three elements keeping them in an inactive state, unable to signal (Bertolotti et al., 2000). However, when unfolded proteins accumulate inside the ER, Bip begins to bind the unfolded proteins instead and, in the process, releases the ER stress-inducing elements that can then begin signaling.

Two alleles of ATF-6 are expressed in mammals, ATF-6alpha and ATF-6beta, which are 90 kD and 110 kD respectively. Both are transmembrane proteins that have

their luminal domain bound to Bip during non-stress conditions as described above. This interaction retains the protein in the ER and prevents its incorporation into COPII vesicles (Shen et al., 2002). After Bip senses stress and releases ATF-6, the transcription factor is incorporated into COPII vesicles and released from the ER. ATF-6 then traffics to the Golgi where successive cleavages result in the active cleavage product which is about 60 kD in size. The processed form of ATF-6 then translocates to the nucleus and binds ATF/cAMP response elements as well as ER stress response elements to initiate transcription of unfolded protein response (UPR) genes (Malhotra and Kaufman, 2007). Activation of these response elements results in the increased expression of folding chaperone proteins, as well as other proteins that help increase the folding capacity of the ER (Schroder, 2008).

IV – Calcium in the secretory pathway

Calcium is a regulator of several membrane fusion events

Constitutive intracellular membrane fusion in the ER to Golgi pathway has been shown to require calcium. Chelation of cellular calcium results in cargo not reaching the Golgi (Beckers and Balch, 1989). Calcium is also required for yeast vacuole fusion (Peters and Mayer, 1998), fusion of early endosomes (Colombo et al., 1997), as well as many other cellular membrane fusion events (Burgoyne and Clague, 2003).

The most studied calcium-dependent membrane fusion event is neuronal exocytosis. In regulated exocytosis, the SNAREs mediating membrane fusion are assembled, but are arrested before they can initiate membrane mixing. A local calcium

signal is required to enable fusion of the synaptic vesicle with the plasma membrane (Malsam et al., 2008). The molecular sensor for this process is synaptotagmin, a molecule that is not present in the early secretory pathway (Hay, 2007; Tang et al., 2006).

The early conclusion from these results was that calcium is a universal regulator for membrane fusion. However, recent studies have discovered several membrane fusion events that do not have a calcium requirement. Addition of a membrane-permeant chelator to living cells resulted in a block of anterograde as well as retrograde fusion of Shiga toxin B, while at the same time, some known fusion steps were unencumbered (Chen et al., 2002). For example, trafficking from the ER to the ERGIC was not affected, while trafficking from the ERGIC to the Golgi was. Further, early results showing a calcium requirement for yeast vacuole fusion have been challenged (Starai et al., 2005). The study by Starai et al. shows that the inhibitory effect of BAPTA on vacuole fusion can be explained by the ionic strength of the molecule alone, rather than its ability to chelate calcium. The ionic BAPTA molecule acts by extracting peripheral membrane proteins.

Basal cytosolic free calcium concentration is at about 60 nM in the cell, while calcium sensors implicated in synaptic membrane fusion have estimated sensitivities between 1 μM and 10 μM. For other intracellular fusion events, the calcium requirements are not as clearly defined. In many cases, it has not been established whether the calcium requirement for fusion is basal or an elevated local burst. Inhibition with chelators may just mean that free calcium levels at or near 100 nM are required for fusion to not be impaired, as chelation is not easily calibrated inside cells.

There are several intracellular fusion events that are sensitive specifically to fast chelators, but are not impaired by the presence of equal amounts of a slower chelator that take longer to reach equilibrium (Burgoyne and Clague, 2003). In these cases, it is likely that membrane fusion requires a local calcium pulse above steady state calcium levels (Adler et al., 1991) or requires calcium sensors near a source of a continuous calcium leak (Hay, 2007).

The endoplasmic reticulum is the primary cellular storage compartment for calcium

The primary calcium storage compartment in the cell is the ER. The majority of calcium in the ER is bound by calcium-binding proteins, with the free calcium in the ER estimated to be as high as 0.7 mM (Bygrave and Benedetti, 1996; Meldolesi and Pozzan, 1998; Montero et al., 1995). Including calcium sequestered by proteins in the lumen of the ER, the total calcium concentration is estimated to be more than 1 mM (Foskett et al., 2007). Regulated calcium release from the ER happens through Inositol 1,4,5-trisphosphate (IP3) receptors or ryanodine receptors, which are transmembrane channels located in the ER membrane.

IP3 receptors are a diverse family of transmembrane proteins that allow calcium to leave the ER upon activation. IP3 receptors are activated by binding of IP3. IP3 is a soluble second messenger molecule that is generated at the plasma membrane by phospholipase C (Alberts et al., 2008). After activation the channel provides a pathway for calcium to follow its electrochemical gradient and diffuse from the ER into the cytoplasm. This process results in calcium clouds near the channel in which the calcium concentration can be as high as 1 μM, while distances as close as 1 μm away from the

channel may have calcium concentrations 100 times lower (Foskett et al., 2007). A model of such a calcium cloud is shown in Figure 4 (Foskett et al., 2007). Because IP3 receptor activation is highly regulated the calcium signal leaving the ER can be decreased and amplified depending on receptor activation. This allows the receptor to generate a diverse set of calcium signals on the outside of the ER.

Calcium chelators

All of the studies that have investigated the role of calcium in ER to Golgi transport have relied on calcium chelators, primarily 1,2-bis(2-aminophenoxy)ethane-N,N,N',N'-tetraacetid acid (BAPTA) and ethylene glycol tetraacedic acid (EGTA). BAPTA and EGTA are structurally very similar molecules (Figure 5). Each of these molecules can bind four calcium ions, one with each of its four carboxylic acid groups and both have the same affinity for calcium. The only structural differences between the two molecules are the two aromatic rings that are present on BAPTA, but not EGTA. This small structural change results in a lower rate constant in EGTA for calcium binding. That means that calcium quenching happens about one thousand times faster with BAPTA than with EGTA in otherwise equal conditions (Adler et al., 1991; Burgoyne and Clague, 2003). However, it is also possible that effects of BAPTA on membrane fusion are a product of its proximity to the plasma membrane, due to its aromatic rings. In cases in which BAPTA, but not EGTA inhibit fusion it is likely that a highly localized calcium pulse acts in a regulatory fashion in this membrane fusion event. This is the case because a calcium pulse will diffuse very quickly in the cytosol.

While the fusion steps within the secretory pathway are well defined, the roles for calcium have not been established. Because this is such a physiologically important pathway, it is going to be necessary to understand the regulatory aspects of ER to Golgi transport as well as possible. Calcium plays important regulatory roles in many membrane fusion events, as outlined above. My hypothesis is that luminal calcium plays a regulatory role in ER to Golgi transport that previous studies have failed to elucidate. Calcium may act as a negative regulator for COPII vesicle fusion on the way to the ER. Calcium may also act in the intermediate compartment and regulate cargo sorting events that happen there. Cargo sorting in the intermediate compartment is poorly understood at present. Elucidating a role for calcium in this compartment will give us a better understanding of these important sorting events. Better knowledge of protein sorting in the intermediate compartment could become useful in the development of protein drugs, as well as in trafficking diseases.

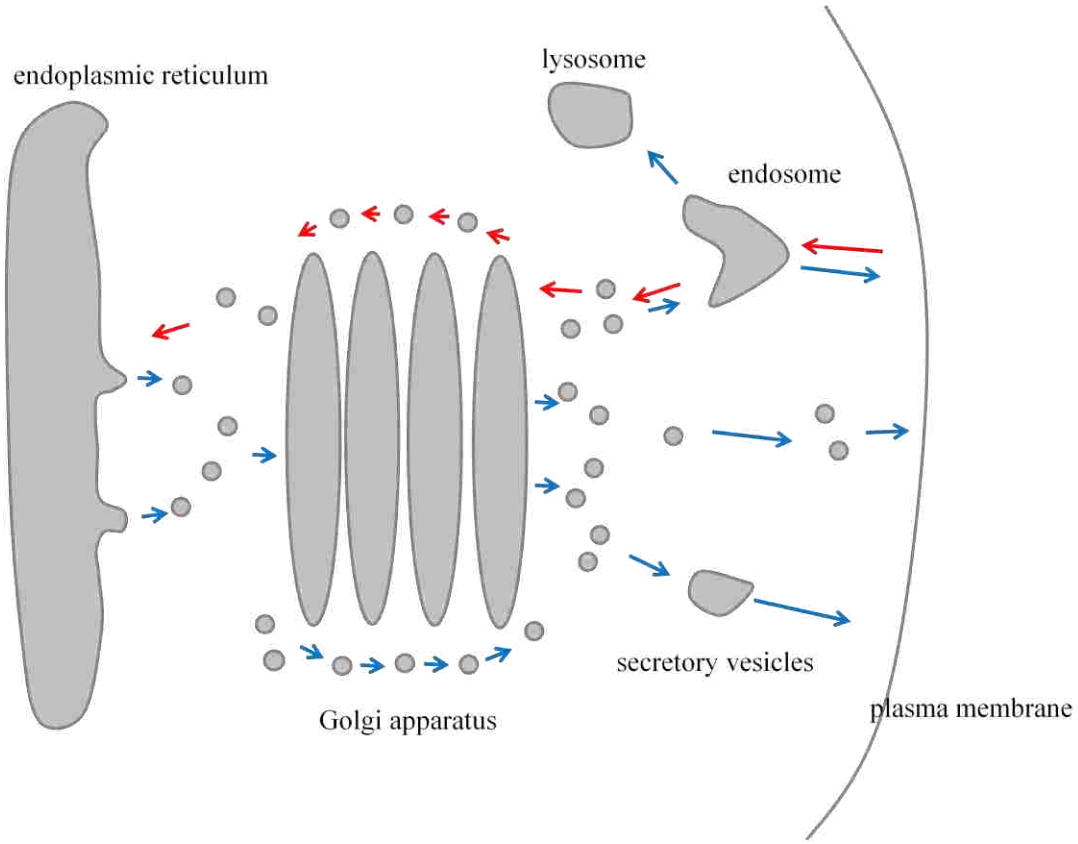

Figure 1—The secretory pathway.

This diagram shows all of the compartments of the secretory pathway. Proteins are folded and glycosylated in the endoplasmic reticulum. This is followed by trafficking to the Golgi apparatus, where final protein modifications occur. After that the cargo is transported to its final destination, which is one of several available compartments, including the lysosomes, different endosomes, the plasma membrane, or the extracellular space.

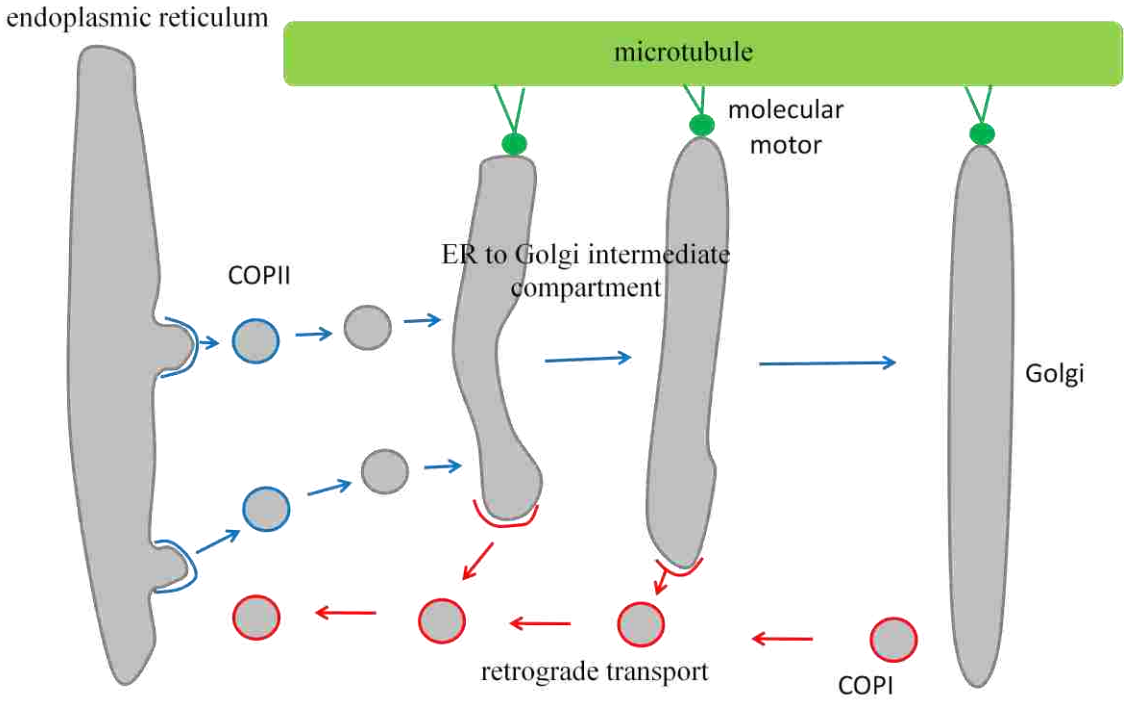

Figure 2 – Endoplasmic reticulum to Golgi transport leads through the ER to Golgi intermediate compartment.

This Figure shows the location of COPII and COPI coats between the ER and the Golgi. COPI is responsible for retrieving ER proteins from the ERGIC, as well as from the Golgi apparatus. COPII buds vesicles from the ER. These vesicles form the ERGIC, which then attaches to microtubules and is moved towards the Golgi by motor proteins.

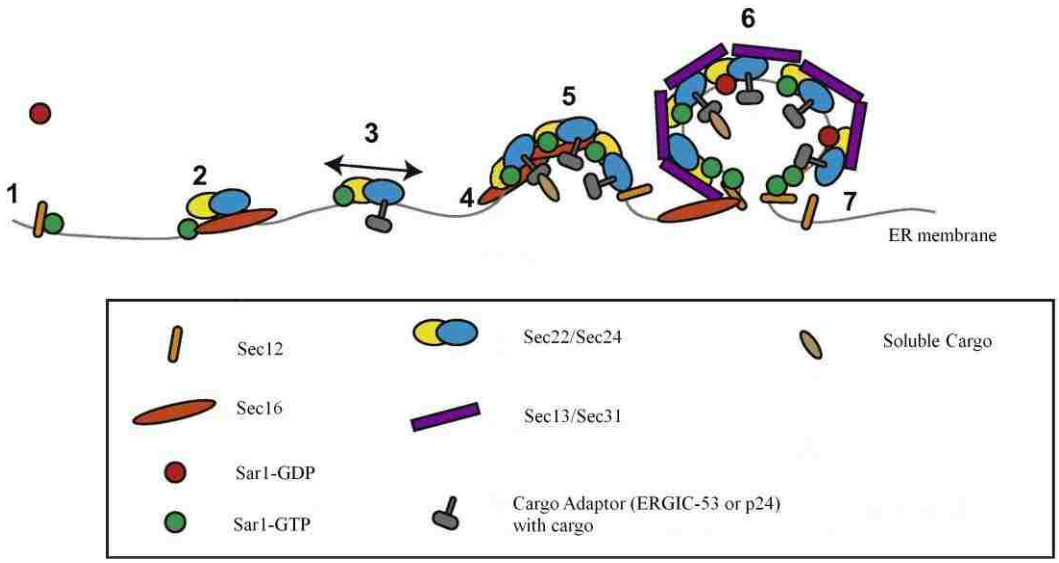

Figure 3– Schematic of COPII vesicle formation (adapted with permission from Budnik and Stephens, 2009)

Step 1: Sec12 recruits and activates Sar1. Step 2: Sec16 and Sec23/Sec24 are recruited by Sar1. Steps 3 and 4: Sec23/Sec24 binds adaptor proteins to concentrate cargo. Step 5: Inner coat proteins form the first COPII shell. Step 6: Sec13/Sec31 is recruited to from the outer shell. Step 7: The complete coat is assembled and the vesicle is ready to bud off.

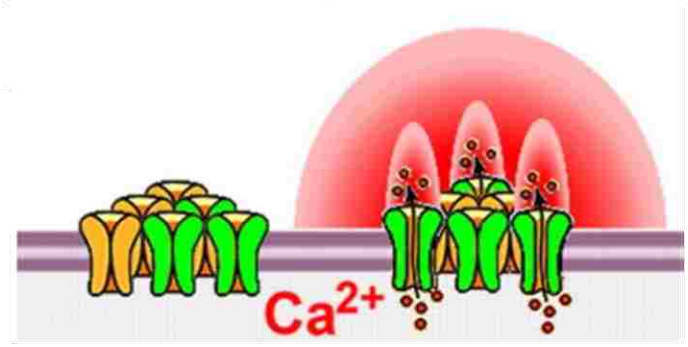

Figure 4 – Calcium puffs can elevate local calcium concentrations (adapted with permission from Foskett et al., 2007)

This schematic representation shows that channels in the ER membrane can generate local areas with a high calcium concentration.

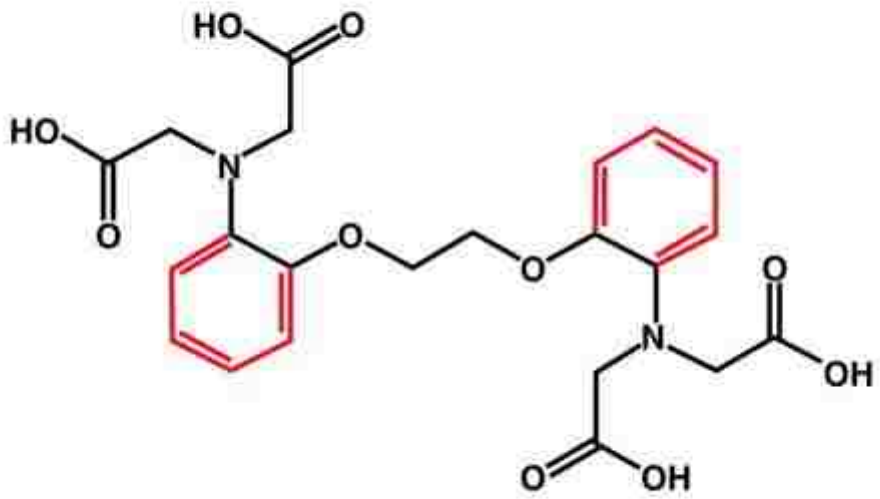

Figure 5 –Chemical structures of EGTA and BAPTA

BAPTA is represented by both black and red lines, while EGTA is represented by the black lines only.

Materials and Methods

Depletion of luminal calcium

Calcium free DMEM (D9802-05B; US Biological, Swampscott, MA) was supplemented with 10% fetal bovine serum (FBS) that had been dialyzed (twice for 2 hours each) in a 100-fold excess of calcium-free phosphate-buffered saline (PBS). Cells to be depleted of luminal calcium were washed twice with calcium-free DMEM/10%FBS containing 10 µM cyclopiazonic acid (CPA; C1530, Sigma-Aldrich, St. Louis, MO), 1 mM EGTA or 0.3 mM EGTA, and 25 mM Hepes, pH 7.2, and then incubated in that medium for 15 minutes. This was followed by an incubation (usually 15 minutes) in calcium-free DMEM/10%FBS, no CPA, 0.3 mM EGTA, and 25 mM HEPES, pH 7.2. Some treatments did not include HEPES in the buffer or included 10 µg/mL cycloheximide for a 30-min period before addition of CPA; in these cases, cycloheximide was also maintained in the medium during the CPA treatment and subsequent calcium-free chase. A 40 minutes cycloheximide pretreatment has been shown to block ATF-6 activation by thapsigargin in HeLa and COS cells (Haze et al., 1999).

For 15°C treatment, cells were incubated for 30 minutes at 15°C in DMEM supplemented with 10% FBS and 25 mM HEPES (pH 7.2).

Immunofluorescence

For immunofluorescence, cover slips were dropped directly into well of room temperature 4% paraformaldehyde in 0.1 M sodium phosphate, pH 7.0, for 30 minutes. Samples were then quenched twice for ten minutes with 0.1 M glycine in PBS. Cell

permeabilization was carried out for 15 minutes at room temperature by using permeabilization solution (0.4% saponin, 1% bovine serum albumin (BSA), and 2% normal goat serum in PBS), followed by incubation in primary antibodies diluted in permeabilization solution for 1 h at room temperature. After three rigorous washes with permeabilization solution, the cover slips were incubated with secondary antibodies diluted in the same buffer for 30 minutes, followed by three more washes. For immunofluorescence of Sec16, cover slips were washed with PBS and then fixed for 10 minutes at -20°C in 100% methanol, and the antibody incubation/wash solution was PBS, pH 7.5, with 1% BSA. Cover slips were mounted using Vectashield anti-fade solution (Vector Laboratories, Burlinggame, CA) and analyzed using an E800 microscope (Nikon, Tokyo, Japan) with a 60X plan APO numerical aperture 1.40 objective. Images were collected using an ORCA 2 digital camera (Hamamatsu, Bridgewater, NJ) controlled by OpenLab software (Improvision, Coventry, United Kingdom). Images for quantification were collected in a consistent manner with regard to cell morphology, protein labeling intensities, and exposure. After choosing a fixed exposure time for each color channel that would accommodate the majority of cells, I avoided any cells whose intensity values in any color exceed the saturation value of 16383 or fell below 4000 on our 14 bit acquisition system. I also avoided capturing cells lacking a flat morphology and single, well-defined nuclei surrounded on all sides by an expanse of cytoplasm. Only cells exhibiting relatively strong and clear antibody labeling were selected. An image stack was collected for each color channel for each field of cells randomly encountered containing at least one cell that met the necessary objective criteria for quantification.

Quantification of Images

Separate excitation and emission filter wheels equipped with fluorescein isothocyanate (FITC) and cyanine (Cy) 3 and Cy5 were used. For quantification of rbet1 and p24 objects, 21 images were captured in 200 nm increments. Images were deconvolved using Huygens Essential Widefield software (Scientific Volume Imaging, Hilversum, The Netherlands). For a given field, a single image plane containing rbet1 or p24 labeling in focus in the peripheral cytoplasm was selected, and the background labeling was removed by defining a dark extracellular area of the image as zero using the automation tool in OpenLab. An rbet1 or p24 object binary image mask was generated by thresholding rbet1 labeling at four times over its intensity in a peripheral area lacking punctate objects (i.e., the labeling of rbet1 or p24 in the ER). A Golgi mask was then created by thresholding the GM130 or GPP130 labeling at 25% of its maximum intensity. The Golgi mask was subtracted from the rbet1/p24 object mask using Boolean operations to generate a peripheral rbet1 object mask; this mask was used to identify and quantify pixels within peripheral rbet1 or p24 objects.

For measurement of ER to Golgi transport a single widefield plane was collected for each color channel. Images were not deconvolved. Background was removed by defining a dark extracellular area of the image as zero using the automation tool in OpenLab. The Golgi markers GM130 or GPP130 were then used to generate a Golgi mask. The ER mean value was derived by drawing an ROI in the peripheral area of the cell, usually close to the nucleus but on the side of the nucleus opposite to the Golgi apparatus. The mean value of the ER ROI and the maximum value of the Golgi mask

were used to generate the transport index. Each data point in these experiments includes at least 20 quantified cells.

To measure bulk flow ER to Golgi transport HeLa cells stably expressing the Ariad regulated secretion domain fused to GFP were grown on cover slips in the presence of 1 µg/mL puromycin (Rivera et al., 2000). Throughout the experiments, culture medium was maintained at 37°C. Cells were calcium-depleted as described above with 15 minutes of CPA treatment followed by 15 minutes in calcium-free medium. Cover slips were then placed into medium containing 1 mM AP21998 and 10 µg/mL of cycloheximide. Cover slips were then fixed and stained with GPP130 as described above. Images were quantified to generate the transport index.

Brefeldin A recovery assay

NRK cells were grown at 37 °C on cover slips and were treated for 30 minutes with 2.5 µg/mL brefeldin A. CPA-treated cells were switched to calcium-free DMEM/10%FBS with 0.3 mM EGTA and containing 10 µM CPA in the presence of 2.5 µg/mL of BFA, while control cells were incubated for 15 extra minutes with 2.5 µg/mL BFA. Cover slips were then washed twice with either calcium free DMEM/10%FBS or control medium to remove the BFA. CPA-treated cells were then incubated in calcium free DMEM/10%FBS with 0.3 mM EGTA. Throughout the experiment, the medium contained 10 µg/mL of cycloheximide. Cells were then fixed as described above and stained using anti-Mannosidase II antibody (1/1000) followed by anti-FITC secondary antibody. Because Golgi markers are diffuse throughout the cell after BFA treatment, the

maximum ER intensity was used instead of the maximum Golgi intensity to generate a transport index at the early time point.

ATF-6 detection

NRK cells were transfected with FLAG-ATF-6. Two days after electroporation, cells were washed once with PBS and once with swell buffer (10 mM HEPES 7.4, 10 mM KCl, 1.5 mM $MgCl_2$, 0.5 mM EDTA, 0.5 mM EGTA, 1 mM DTT, and protease inhibitors (ALLN, PMSF, leupeptin, pepstatin, and aprotinin)). Cells were then incubated on ice for 10 minutes in 1 mL swell buffer. The plates were scraped and clles were passed through a syringe 15 times using a 22G needle. After centrifugation at 1000 x *g* for 10 minutes the pellet containing total membranes was collected and analyzed using SDS-PAGE electrophoresis (8.5% acrylamide) and Western blotting using anti-FLAG and anti-calnexin antibodies.

VSV-G trimer immunoprecipitation

NRK cells were transfected with VSV-G-myc or VSV-G-GFP and incubated for 24 h at 40°C. Cells were calcium depleted as described above and released in medium at 32°C. Cells were incubated with cold 25/125 buffer (25 mM HEPES, pH 7.2, 125 mM potassium acetate) with 1% TX-100, and protease inhibitors (pepstatin, leupeptin, aprotinin) and incubated for 10 minutes at 4°C. After this, the cells were scraped and incubated end over end for at last 10 minutes at 4°C. The insoluble fraction was removed by centrifugation at 15000 x *g* for 15 minutes. The supernatant was then added to Protein A beads that had been incubated for at least 1 h with I14 hybridoma medium and then

had been washed at least 4 times with 25/125. These were incubated for 2 h end over end at 4°C and washed three times with 25/125. Samples were then analyzed using SDS-PAGE electrophoresis and Western blotting for either GFP or myc.

Antibodies

Monoclonal anti-rbet1 antibodies were described previously (Hay et al., 1998). Affinity purified polyclonal anti-p24, -Sec23, and –βCOP from our laboratory were described previously (Bentley et al., 2006). Anti-Sec31 was produced in rabbits against the synthetic peptide KLKEIDRTAMQAWSPAQNHPC and then affinity purified using a column of the immobilized peptide. Anti-GM130 and anti-p115 were a gift from Dr. Martin Lowe (University of Manchester, Manchester, United Kingdom). Anti-Sec16 antibody (KIAA0310) was acquired from Novus Biologicals (Littleton, CO). Anti-GPP130 antibody (PRB144C) was purchased from Covance Research Products (Princeton, NJ). Anti-Mannosidase II (MMS-11-R-200) antibody was purchased from Covance Research Products. Anti-myc monoclonal antibody 9E10 was purified from hybridoma tissue culture supernatant. Anti-GFP antibody (MMS-118P) was purchased from Covance Research products. Anti-Syntaxin 5 antibody was previously described (Williams et al., 2004). Anti-Calnexin (SPA-865) antibody was purchased from Stressgen (Ann Arbor, MI, USA). Anti-FLAG antibody (F1804) was purchased from Sigma-Aldrich (St. Louis, MO, USA). Secondary antibodies were FITC, Cy3, or Cy5-conjugated and purchased from Jackson ImmunoResearch Laboratories (West Grove, PA).

Luminal calcium measurements

Normal rat kidney (NRK) cells (~80% confluent) were transiently transfected with 1.5–2 µg of purified plasmid DNA of the respective calcium sensor using TransFast (Promega, Vienna, Austria) as described previously (Trenker et al., 2007). Cells were used for experiments at 48 h after transfection. YC3.6 (Nagai et al., 2004) and YC2.1 (Miyawaki et al., 1997) were used to monitor the free calcium concentration in the cytosol, and D1ER (Palmer et al., 2004) was used to monitor free calcium within the ER lumen (Malli et al., 2005; Osibow et al., 2006). The fluorescence resonance energy transfer-based calcium sensor D1ER was excited at 440 ± 21 nm (440AF21; Omega Optical, Brattleboro, VT), and emission was collected simultaneously at 535 and 480 nm with a single camera using an optical beam splitter (535 and 480 nm, Dual-View MicroImager; Optical Insights, Visitron Systems, Puchheim, Germany). $[Ca^{2+}]$Cyto was calculated from the normalized ratio values $Ratio_i^n = \left(\frac{(F_i^{535}/F_i^{480})}{(F_0^{535}/F_0^{480})} \right)$ using the following equation: $[Ca^{2+}] = K_D \cdot \left(\frac{Ratio_{i^n} - Ratio_{min}}{Ratio_{max} - Ratio_{i^n}} \right)$ µM (Osibow et al., 2006). The K_D value for YC3.6 was assumed to be 250 nM (Nagai et al., 2004). For the calculation of $[Ca^{2+}]_{ER}$, the raw D1ER recordings (*Ratio* F^{535}/F^{480}) were corrected for bleaching using a calculated individual bleaching-function (R0) by subtracting R0 from the raw *Ratio* F^{535}/F^{480}. From this curve the respective $Ratio_i$, $Ratio_{min}$, and $Ratio_{max}$ values were extracted and $[Ca^{2+}]_{ER}$ was calculated using the equation above. The K_D value of D1ER *in situ* for calculating $[Ca^{2+}]_{ER}$ was assumed to be 220 µM according to Rudolf et al., 2006. $Ratio_{min}$ and $Ratio_{max}$ were determined using 1 µM ionomycin in 1 mM EGTA and subsequently in 2 mM Ca^{2+}-containing solution, respectively, for each single measurement (cytosolic Cameleons and D1ER). Statistical data for calcium

measurements are presented as mean ± SEM. Analysis of variance and Scheffé's post hoc F test were used for evaluation of the statistical significance, with $p < 0.05$ defined as significant.

Heterotrimerization fusion assay

COPII vesicle fusion experiments were carried out as described previously (Bentley et al., 2006; Cai et al., 2007b; Xu and Hay, 2004). In brief, the vesicular stomatitis virus-glycoprotein (VSV-G)-myc expressing NRK and pulse radio-labeled VSV-G* containing cells were permeabilized by scraping with a rubber policeman and then washed and resuspended at ~170 µL per 10 cm plate in 50/90 buffer (50 mM HEPES, pH 7.2, and 90 mM potassium acetate). A first stage (vesicle release) incubation to produce enough vesicles for a 24-point fusion assay contained 1.96 mL and consisted of 432 µL of water, 67.5 µL of 0.1 M magnesium acetate, 135 µL of ATP regenerating system, 40.5 µL of 1M HEPES, pH 7.2, and 270 µL of weak calcium buffer (20 mM Hepes, pH 7.2, 1.8 mM $CaCl_2$, and 5 mM EGTA), 675 µL of dialyzed rat liver cytosol, and 337.5 µL of either of the permeabilized cell populations. After incubation at 32°C for 30 minutes to allow vesicle release, cells were removed by centrifugation at 4000 x *g* for 1 minute followed by 14,000 x *g* for 1 minute. The supernatant, which contains released COPII vesicles, was saved. For the second stage fusion incubations each reaction totaled 200 µL and contained 72.5 µL of VSV-G-myc vesicles, 72.5 µL of VSV-G* vesicles, and 55 µL of 25/125 buffer (25 mM Hepes, pH 7.2, 125 mM potassium acetate). It was at this point that chelators such as BAPTA and EGTA were added. After a 20 minute pre-incubation on ice with these test components, the reactions were

incubated at 32°C for 60 minutes to allow tethering, fusion, and heterotrimerization between VSV-G-myc and VSV-G* vesicles. For measuring heterotrimers, the final vesicle suspensions were supplemented with 2% Triton X-100, incubated with agitation at 4°C for 20 minutes, and then centrifuged at 100,000 x *g* for 30 minutes. The 100,000 x *g* supernatants containing solubilized VSV-G trimers were then processed for immunoprecipitation by using 5 µg of biotinylated anti-myc antibodies and 5 µL (packed) streptavidin Sepharose (GE Healthcare). Immunoprecipitates were solubilized in SDS sample buffer, analyzed by SDS-polyacrilamide gel electrophoresis (PAGE; 8%), phosphorimaging, and co-precipitated VSV-G* was quantified.

Results

Fast chelation of calcium during *in vitro* COPII vesicle fusion reveals a role for luminal calcium

To test the role luminal calcium may play in the early secretory pathway, I used an established cell-free reconstitution of homotypic COPII vesicle fusion (Bentley et al., 2006; Xu and Hay, 2004). COPII vesicles generated *in vitro* from permeabilized NRK cells possess or recruit all components necessary for efficient tethering and fusion to generate pre-Golgi intermediates resembling cellular vesicular tubular clusters (VTCs) (Xu and Hay, 2004). Membrane fusion and contents mixing is scored biochemically by the heterotrimerization of radioactive VSV-G* with non-radioactive VSV-G-myc present initially in distinct COPII vesicle populations. Heterotrimers are assayed by detergent solubilization of vesicles, followed by immunoprecipitation using a monoclonal anti-myc antibody. Radioactive VSV-G* subunits are then detected by autoradiography. Figure 6 shows that the addition of the fast membrane-impermeant calcium chelator BAPTA resulted in stimulation of heterotrimer production. The increase in heterotrimer formation is dependent on the amount of BAPTA added to the buffer. At 6 mM BAPTA, the fusion increase is almost six fold. Interestingly, addition of the chelator EGTA does not result in an increase in vesicle fusion. EGTA and BAPTA have equal affinities for calcium; however, EGTA takes 1000 fold longer to reach equilibrium than BAPTA (Burgoyne and Clague, 2003). This result suggests that the speed at which BAPTA sequesters the calcium may account for the difference.

The membrane permeant derivatives of BAPTA and EGTA, BAPTA/AM and EGTA/AM were used to test this hypothesis. Both of these contain a hydrophobic amino-methoxy group that allows the molecule to pass through membranes. Figure 7 shows that addition of BAPTA/AM to the *in vitro* fusion assay results in a robust increase of heterotrimer formation. Addition of EGTA/AM mimics the BAPTA/AM very closely (This experiment was conducted by Deborah Nycz though I did the preliminary work). This result implicates the ability of BAPTA to quickly neutralize a calcium gradient as being responsible for the increase of heterotrimer formation. While EGTA/AM and BAPTA/AM inside the vesicle result in roughly equal fusion enhancement, only BAPTA can neutralize the calcium leaking out of the vesicle quickly enough before it interacts with machinery on the outside of the vesicle membrane.

To test whether the dramatic and unexpected effects of BAPTA on fusion were due to calcium chelation as opposed to some other direct action of BAPTA on proteins or membranes, I analyzed the BAPTA sensitivity of fusion in the presence of a different free calcium concentration in the buffer. As shown by black squares in the graph in Figure 8, the presence of excess calcium shifted the BAPTA stimulation curve to the right, delaying stimulation until the BAPTA concentration significantly exceeded that of bulk added calcium. This indicates that calcium-free BAPTA, but not calcium-saturated BAPTA, is an active species in the heterotrimer assay. This is consistent with BAPTA acting, at least in part, through calcium chelation. Importantly, it rules out most nonspecific effects that could be caused by high concentrations of this molecule.

The results described are all compatible with the hypothesis that luminal calcium plays an important regulatory role in COPII vesicle fusion. Chelation of the calcium

results in vesicles that are more fusogenic and produces a robust stimulation in the heterotrimer assay.

Depletion of luminal calcium in intact cells results in an enlarged ER to Golgi intermediate compartment

Because the *in vitro* experiments resulted in changes in COPII vesicle fusion caused by luminal calcium, I decided to develop a way to deplete luminal calcium in intact cells. The calcium gradient between the ER and the cytoplasm is maintained by sarco/endoplasmic reticulum calcium ATPases (SERCA) in the ER membrane. These maintain the gradient by constitutively pumping calcium into the lumen of the ER. Inhibition of these ATPases should result in an accumulation of calcium ions in the cytoplasm. Plasma membrane ATPases can then remove the calcium and transport it into the medium.

I used the drug cyclopiazonic acid (CPA), which is a specific inhibitor of the SERCA pumps in the ER (Mason et al., 1991). To deplete luminal calcium, NRK cells were treated with CPA for 15 minutes in calcium-free medium containing EGTA, followed by 15 minutes without CPA in calcium-free medium with EGTA. The CPA treatment results in depletion of the luminal calcium, while the EGTA can sequester any calcium that is pumped out of the cells. To confirm that the protocol achieved specific depletion of luminal calcium as intended, live cell imaging of luminal and cytosolic calcium were used. Calcium concentrations were determined using transfected chameleon biosensors D1ER (Palmer et al., 2004) and YC3.6 (Nagai et al., 2004) that have optimal affinities for the free calcium concentrations in the respective

compartments. Figure 9 shows that treatment with 10 µM CPA resulted in a severe depletion of ER luminal free calcium within 10 minutes, from 385 µM, a typical resting value for cultured mammalian cells (Malli et al., 2008; Osibow et al., 2006), to 23 µM (calibration of Foerster ratios not shown); this means that vesicular COPII-derived membranes generated from the ER after 10 minutes must also be depleted of vesicular calcium. As expected, cytosolic calcium underwent an extreme increase as the luminal compartment was emptied, but this was cleared and restored to the resting value of 45-50 nM 15 minutes after CPA was added (Figure 10). These data show that by the end of the 15 minute CPA treatment and the start of the chase period, luminal calcium is depleted by more than 90% and cytosolic calcium is at resting levels. Furthermore, this condition seems to remain stable during the chase period after CPA washout. (These experiments were conducted by Ismene Fertshai, Roland Malli, and Wolfgang Graier at the Medical University of Graz following my calcium depletion protocol. For further experimental details on the calcium imaging, please refer to (Bentley et al., 2010))

To observe the effects of luminal calcium depletion on the intermediate compartment, I decided to use the ER-to-Golgi SNARE rbet1, a type II integral membrane protein, as a marker. If subtle changes in membrane flux between the ER and Golgi occurred, rbet1 distribution should be a sensitive indicator, because rbet1 rapidly cycles between the ER and Golgi and is largely localized to the ERGIC at steady state (Hay et al., 1998). Figure 11 shows that CPA treatment results in a change in the distribution of rbet1. Control cells exhibit strong rbet1 labeling in the perinuclear area surrounding the Golgi which is stained for GM130. There are also fainter punctate structures in the peripheral cytoplasm that are not associated with the Golgi apparatus.

CPA-treated cells, in contrast, displayed relatively more intense punctate peripheral rbet1-positive objects compared with the perinuclear labeling. This change did not result from a dispersal of Golgi into the peripheral cytoplasm, as indicated by the GM130 labeling. Also shown in Figure 11, the overall effect of CPA seemed similar to that when the cells were incubated at 15°C, which is a treatment that is commonly used to trap anterograde cargo and vesicle machinery in swollen, peripheral ERGIC structures (Saraste and Svensson, 1991).

The increased peripheral rbet1 staining during CPA treatment can be observed quantitatively by measuring the average area of peripheral rbet1-positive objects over time (Figure 12). The area of an average peripheral rbet1-positive structure more than doubled during the standard treatment condition of 15 minutes CPA plus 15 minutes calcium-free chase. Most of the increase in rbet1 object size occurred during the chase period during which luminal calcium is depleted and cytosolic calcium has returned to resting levels. A further 15 minutes of calcium-free chase resulted in a slight decrease in peripheral object size. However, this apparent decrease is likely an artifact of the gross morphological change in the cells, which began to dissociate from the dish and round up during this interval. I compared the effect of CPA treatment on peripheral object size to other treatment conditions (Figure 13). While incubating the cells at 15°C resulted in a significant increase of peripheral object size, the change caused by CPA treatment was much more dramatic. The 15°C treatment resulted in an about 50% increase of average object size. CPA-mediated calcium depletion resulted in an increase of about 250%. Treating the cells with CPA and cycloheximide resulted in a comparable increase of average object size, indicating that synthesis of new protein is not the cause of the

increase in rbet1 staining, but rather a product of redistribution of already existing protein. Cycloheximide also blocks the accumulation of unfolded proteins during ER luminal calcium depletion and Ire1-dependent transcriptional activation of ER stress response elements (Haze et al., 1999; Ruegsegger et al., 2001). This makes stress responses related to the accumulation of unfolded proteins seem unlikely to be an important determinant of the rapid changes in ERGIC structure observed with CPA. Thapsigargin is a distinct and irreversible SERCA inhibitor. Treating cells with thapsigargin for 30 minutes also resulted in a phenotype indistinguishable from CPA. This confirms the mechanism of the CPA effect.

In order to observe subtle changes in size distribution, I binned peripheral rbet1 objects according to size (Figure 14). Objects were identified by drawing a mask on rbet1. This mask included any rbet1 staining that exceeded four times the ER background level of staining. Although the number of sub-resolution objects remained virtually unchanged in CPA-treated cells, CPA treatment clearly generates a new population of very large objects (>0.45um^2). Interestingly, the 15°C treatment resulted in a different distribution of object sizes than the luminal calcium depletion. There is a large increase in very small objects during 15°C treatment, which exceeds both control and CPA-treated cells. Although 15°C caused an overall increase in the number of objects, most of the increase was in the small and intermediate size objects (<0.45um^2). This suggests that the two different treatments (CPA and 15°C) affect different steps of ER to Golgi trafficking. For example, the CPA effect would be consistent with overactive fusion of COPII vesicles and VTCs, or with defective membrane sorting in the

ERGIC, while the 15°C phenotype would be more consistent with a buildup of vesicles or intermediate compartment objects due to a lack of microtubule-dependent transport.

Total rbet1 labeling intensity increased significantly in the CPA and 15°C treated cells (Figure 15) while total rbet1, as assayed by Western blot, was not affected (Figure 16). This could indicate either that more rbet1 was present after these treatments or that the pool of rbet1 trapped in intermediate structures was more accessible for immunofluorescence labeling. This increase was specific to the particular rbet1 monoclonal antibody that was used (16G6). The GM130 labeling intensity was unchanged in the same cells (Figure 17). In addition, another ERGIC marker, p24, did not change significantly in intensity. The 16G6 antibody that was used for the rbet1 Western blot is a monoclonal antibody that binds the N-terminal domain of rbet1. This suggests that the N-terminus of rbet1 is more accessible in the swollen structures, which might indicate changes in SNARE protein interactions.

To test whether the luminal calcium depletion effect was specific to rbet1 or a general effect on the intermediate compartment, I examined the distribution of another ERGIC marker (Figure 18). p24 rapidly recycles between the ER and the Golgi like rbet1, but is a cargo adaptor and not a SNARE (Belden and Barlowe, 1996; Schimmoller et al., 1995). The distribution of p24 was quantified in the same way as for rbet1 above. Figure 18 shows that p24 also had an increased localization to Golgi-negative punctate peripheral objects upon luminal calcium depletion. This change was reflected quantitatively by a dramatic increase in the number of large p24 objects (>0.45 μm^2) (Figure 19). However, unlike rbet1, there was no significant increase in p24 total integrated staining intensity (data not shown). Taken together, the above results show

that multiple ERGIC markers rapidly accumulate in large peripheral structures upon luminal calcium depletion.

ERES do not change their size in calcium-depleted cells

The enlarged objects clearly represent pre-Golgi intermediates because they do not have any Golgi marker staining. However, it is unclear whether they are part of the intermediate compartment or swollen ERES. To see if there were any obvious changes to ERES, I stained calcium-depleted cells for the ERES marker Sec16. Sec16 is a large protein that is involved in ERES formation, but, unlike the coats, it is not loaded onto COPII vesicles (Budnik and Stephens, 2009). Figure 20 shows cells stained for rbet1 as well as Sec16. While-calcium depleted cells have a significantly altered distribution of rbet1, Sec16 staining remains unchanged. Figure 21 shows the quantification of the peripheral rbet1 and Sec16 objects in the same cell population. While there is a significant increase of above threshold rbet1 objects, the number of Sec16 objects remains unchanged.

If the swollen rbet1 structures were ERES, then the ERES marker Sec16 would likely change its distribution in a similar pattern. Because Sec16 remains unchanged, it is likely that the swollen structures are post-budding objects. However, if these are early objects in the intermediate compartment, they would still be closely associated with the ERES. To identify how closely to the swollen rbet1 structures were associated with ERES, the five largest rbet1 structures in each cell, those most likely to be created as a specific result of calcium depletion, were analyzed in more detail. In 98% of all cases these rbet1 objects overlapped by at least 50% of their area with a Sec16-positive object

(Table 1). A similar experiment was carried out using rbet1 and β-COP. β-COP is a subunit of COPI, which is the coat responsible for retrograde transport from the Golgi. In 73% of all cases, the largest peripheral rbet1 objects overlapped by at least 50% of their area with a β-COP positive object (Table 1). Overlap with beta-COP is expected because COPI vesicles are formed at the ERGIC to retrieve wayward ER proteins. The majority of all objects are positive for both COPI as well as ERES markers.

Because of the lack of change to Sec16 and the presence of both COPI and ERES markers on the swollen structures, the most likely conclusion is that the large rbet1 objects are post-budding, early intermediate compartment structures.

VSV-G trafficking can be measured using intact cells and fluorescence microscopy

The results described above indicate that luminal calcium plays a role in maintaining the structure and organization of the secretory pathway. However, these experiments do not address whether the primary function of the secretory pathway, the trafficking of proteins, is dependent on luminal calcium. It is conceivable that the changes in morphology do not affect trafficking of cargo through the system. The more likely hypothesis however is that the changes we observed in secretory pathway morphology result in trafficking deficiencies. In order to test this hypothesis, I developed a morphologically intact cell assay that allows the measurement of ER to Golgi transport kinetics. As cargo, I used transiently transfected VSV-G-GFP. After transfection VSV-G remains confined to the ER by maintaining the cells at 40°C. This allows VSV-G-GFP production to continue while it accumulates in the ER. After a temperature shift to the permissive 32°C, VSV-G-GFP travels to the Golgi apparatus. The cells are then fixed

and I measured the amount of VSV-G-GFP that had traveled from the ER and arrived at the Golgi by image analysis. A region of interest in the ER, free of punctate staining was selected to generate a mean ER value. After that, a mask was generated for the Golgi marker GM130. The maximum VSV-G-GFP intensity for this mask was used together with the ER mean value to generate the transport index. The ratio of Golgi maximum to ER mean provides a quantitative value representing the arrival of VSV-G-GFP in the Golgi apparatus.

To confirm that the assay was capable of measuring changes in VSV-G trafficking, it was necessary to generate a cargo block that was independent of calcium. To impair ER to Golgi trafficking, I chose to knock down the ER to Golgi SNARE Syntaxin 5. Syntaxin 5 is one of the four ER to Golgi SNARES. Previous experiments in this laboratory have shown that addition of anti-Syntaxin 5 antibody to the COPII vesicle heterotrimer assay results in strong inhibition of the fusion signal (Bentley et al., 2006). To knock down Syntaxin 5, NRK cells were transfected with Syntaxin 5 siRNA. To confirm the absence of Syntaxin 5, cells were lysed in sample buffer and analyzed using SDS-PAGE gel electrophoresis followed by Western blotting. Figure 22 shows that the Syntaxin 5 siRNA treatment resulted in a very efficient knockdown (KD) of the protein. Equal amounts of protein were loaded in the Syntaxin 5 KD and the control lanes. I also loaded different dilutions of mock transfected cells. The Western blot shows that Syntaxin 5 was knocked down more than 90%, which should prove more than sufficient to register a trafficking effect.

One day before the experiment both Syntaxin 5 knockdown and mock-treated populations were transfected with VSV-G-GFP. Cells were incubated at 40°C to build

up VSV-G-GFP in the ER. To allow VSV-G-GFP trimerization, but prevent COPII vesicle budding, cells were incubated at 10°C for one hour; this temperature is permissive for folding but not vesicle budding. Before starting the time course, at 10°C the cargo is located diffusely throughout the ER and there is no morphological difference between control cells and Syntaxin 5 depleted cells. After switching the temperature to 32°C the cargo is released from the ER and starts moving towards the Golgi. Three minutes after release from the ER, VSV-G-GFP is beginning to arrive in the Golgi of control cells, but not in Syntaxin 5 depleted cells. After 7 minutes some of the cargo has made it to the Golgi in both populations, but significantly more has accumulated in the control cells.

For each cell a "transport index" value was generated by using a ratio of Golgi maximum and ER mean. These values are then averaged to generate a point on the graph in Figure 23. The graph shows that this quantification method can sensitively measure kinetic changes in VSV-G-GFP transport to the Golgi. Transport of VSV-G-GFP in the cells with knocked down Syntaxin 5 was significantly impaired when compared to mock transfected cells.

To test the effect of luminal calcium depletion on VSV-G transport, cells were either mock-treated or CPA-treated at 10°C. After that, VSV-G-GFP was released from the ER at 32°C. While this experiment showed no effect of CPA treatment when compared to the mock (data not shown), it is possible that calcium depletion requires different conditions at 10°C. Cells treated with CPA at 10°C did not show the morphological changes to the ERGIC structures. There were no enlarged peripheral rbet1 structures in these cells. Because I did not confirm whether the calcium depletion was effective, it is not easy to evaluate such data. However, if the calcium depletion was

effective at 10°C, then any trafficking defect is dependent on the morphological changes to the ERGIC.

VSV-G trafficking in intact cells is impaired at a post-folding stage by luminal calcium depletion

To test kinetic effects of luminal calcium depletion on ER to Golgi transport cells were transfected with VSV-G-GFP and cultured at 40°C. Calcium depletion was performed at 40°C, a temperature at which the treatment causes ERGIC expansion (not shown). After the usual CPA treatment, cargo was released in calcium-free medium at 32°C. Cells were fixed and then VSV-G-GFP transport was evaluated as previously described. Figure 24 shows the quantified results. It very clearly shows that there is a retardation of transport in CPA-treated cells. This result supports the hypothesis that luminal calcium plays an important role in the trafficking of cargo through the early secretory pathway. However, this experiment does not rule out a slowdown caused by folding defects on ER to Golgi transport. It is possible that the lack of luminal calcium results in slower formation of VSV-G trimers and that this causes a slowdown in transport.

To assess this possibility, I measured the formation of VSV-G trimers. Cells were transfected with VSV-G-myc. After calcium-depletion cells were switched to 32°C and then lysed using 1% TX-100. VSV-G trimers were immunoprecipitated using the trimer-specific monoclonal antibody I14 (Nehls et al., 2000). Trimers were then analyzed by SDS-PAGE electrophoresis and Western blotting. Figure 25 shows the quantification of three such experiments. After three minutes at 32°C, VSV-G in both CPA-treated and

control cells reaches its maximum folding level and remained constant. This is consistent with VSV-G folding occurring rapidly, which has been observed previously by others (de Silva et al., 1990). This result suggests that the kinetics of trimer formation are not affected by calcium depletion. During luminal calcium depletion, the speed at which VSV-G folds into trimers is not any slower than it is in control cells. However, the percentage of total VSV-G that folds into trimers seemed generally lower in calcium depleted cells, but was not statistically significant. While it is likely that both populations have a pool of protein that remains unfolded in the ER for the duration of the experiment, it seems that more VSV-G moves into or remains in this pool during calcium depletion. This was also apparent in the total I14 immunofluorescence signal attained following a shift to 32°C (data not shown). Nonetheless, the experiment in Figure 25 suggests that slower protein folding due to luminal calcium depletion is not responsible for the kinetic decrease of ER to Golgi transport. However, this experiment does not rule out the possibility that an increased pool of VSV-G-GFP that is stuck in the ER is responsible for a higher mean ER value in the fluorescence based assay. Because the quantification uses a denominator value derived from the ER, increasing the VSV-G-GFP that is stuck in the ER could result in a diminished transport index. This would mean that the trafficking defect was simply an artifact of less VSV-G-GFP being released into the secretory pathway, rather than a true effect on the post-folding secretory machinery.

To differentiate folding effects from an actual decrease of cargo transport, VSV-G-GFP was transfected into NRK cells and the cells had their luminal calcium depleted as described previously. After fixation, the cells were stained using the VSV-G trimer specific antibody I14. Using this antibody removes any effects caused by unfolded VSV-

G, as only folded VSV-G, which is going to traffic, is measured. In addition, new trimers do not continue to form after the first few minutes (Figure 25). Trimer transport was analyzed as before, both for VSV-G-GFP as well as for I14 staining. In order to prevent effects of newly translated cargo, cycloheximide was added to the cells upon cargo release. Figure 26 shows the quantification of transport of both VSV-G-GFP (Figure 26 A) as well as VSV-G trimers (Figure 26 B) inside the same cells. The VSV-G-GFP signal closely follows the previously observed trend. The previous experiment showed that three minutes after release, all VSV-G is folded. In this experiment, no VSV-G has made it to the Golgi yet after three minutes, shown by the equal transport indices. Ten minutes after release, VSV-G is arriving in the Golgi, continuously increasing until 20 minutes. The trimer only quantification shows the same trend. Both conditions are the same three minutes after release, but starting at ten minutes, VSV-G starts accumulating much faster in the Golgi in the control cells than in the calcium-depleted cells. Curiously, the maximal transport indices are much higher for the trimer-only analysis than they are for the GFP analysis. This shows that a significant amount of VSV-G-GFP remains in the ER, even in untreated cells. However, when using the I14 antibody, the ER values are reduced very close to background indicating that almost all trimerized VSV-G leaves the ER and moves to the Golgi. Alternatively, it is possible that this difference in transport index is the product of a non-linear signal in the antibody binding. Because the amount of trimerized VSV-G remains constant after three minutes, this experiment shows that there is a significant retardation of ER to Golgi trafficking that is not an artifact generated by an increase of unfolded cargo remaining unfolded in the ER.

Golgi reformation after brefeldin A treatment is impaired in calcium depleted cells

Because all trafficking experiments thus far are based on the same cargo, I used a different, non-folding dependent assay for ER to Golgi transport. Brefeldin A (BFA) is an antibiotic produced by a fungus that acts by collapsing the Golgi back into the ER (Lippincott-Schwartz et al., 1989). BFA acts on the GEF for the COPI GTPase ARF1. It prevents the budding of COPI vesicles from the Golgi. This allows SNAREs on the Golgi to become exposed allowing whole Golgi cisternae to fuse with the ER (Nebenfuhr et al., 2002). This does not affect the folding state of Golgi proteins, but takes already existing proteins and moves them to the ER. Washing out BFA then allows these proteins to leave the ER and reform the Golgi. For this experiment, cells were treated with 2.5 µg/mL of BFA for 45 minutes. In the CPA-treated cells, luminal calcium was depleted for the final 30 minutes of BFA treatment. BFA was then washed out and the cells were fixed at each time point. After fixation the cover slips were stained for Mannosidase II, a Golgi-resident enzyme. Treatment with cycloheximide throughout the experiment ensured that only already existing proteins were involved in the reformation of the Golgi. The images were then analyzed similarly to previous experiments, with a Golgi maximum in the periphery that was compared to an ER mean. A similar experiment had been previously conducted in the laboratory by Ting Wang, however the quantification methods had not been refined at that point. At the zero minute point Mannosidase II is diffuse throughout the ER and there is no Golgi marker in the periphery to evaluate. In that case, the maximum ER value was used. The experiment is quantified in Figure 27. The graph shows that the reformation of the Golgi is consistently slower in the CPA-treated cells than it is in the control cells. Even after a full hour of

washout the Golgi reformation is still significantly lagging in the CPA-treated cells, while the control cells have a transport index value that is near the value of untreated cells, and supports the conclusion of the VSV-G trafficking experiments.

Bulk soluble cargo transport in HeLa cells is not affected by luminal calcium depletion

Both VSV-G and the BFA washout experiments relied on membrane protein trafficking to the Golgi. To test a luminal cargo, HeLa cells stably expressing GFP attached to a conditional aggregation domain were used (Gordon et al., 2010; Rivera et al., 2000). This domain clusters newly translated protein in the ER until a target drug is introduced that releases the cargo (Figure 28). These cells were calcium depleted as above and showed a similar phenotype in which peripheral p24 staining puncta were enlarged (Figure 29). After calcium depletion, cargo was released by introducing the drug and transport to the Golgi was measured by the same algorithm as before. Figure 30 shows that the kinetic trajectory of ER to Golgi transport for this cargo was not affected by the depletion of luminal calcium. To confirm that luminal calcium depletion does not affect the rate of drug induced de-aggregation, ER intensities of GFP were measured in each cell. The ratio of maximum ER to minimum ER was generated as a way of measuring aggregates. Figure 31 shows that de-aggregation is rapid when compared to transport. Therefore the transport index is not measuring de-aggregation. That luminal calcium does not affect bulk flow transport is an intriguing result because it suggests that the previously observed effect is not as simple as a general slowdown in ER to Golgi trafficking. Because soluble cargo does not seem to be affected by the CPA treatment,

but membrane proteins (Figure 23) or membrane compartments (Figure 14) are, it is possible that there is a effect on sorting in the ERGIC (see discussion).

Luminal calcium depletion does not result in ATF-6 unfolded protein response activation

Because calcium plays an important role in protein folding inside the ER, it is possible that depletion of calcium results in activation of the unfolded protein response (UPR) (Malhotra and Kaufman, 2007). In that case, signaling activated by the UPR could account for changes in trafficking between the ER and the Golgi. This would be different from calcium directly affecting the fusion machinery. One of the three major pathways that are activated by the UPR is the transcription factor activating transcription factor 6 (ATF-6). Upon ER stress the 98kD ATF-6 gets transported to the Golgi apparatus. Here, it is cleaved by two proteases, which results in a 60 kD size fragment. The cleaved form of ATF-6 then is transported to the nucleus where it activates transcription of stress related genes (Schroder, 2008).

A previous paper in fact showed that VSV-G trafficking defects were caused by activated UPR (Amodio et al., 2009). Two hours of thapsigargin treatment in the presence of normal extracellular calcium resulted in the accumulation of anterograde cargo in the ER and at ERES. Those experiments also resulted in stress-induced morphological changes, such as Golgi fragmentation, that were not present in the studies described here. The CPA conditions I used are relatively mild, because they would not have resulted in extremely high cytosolic calcium over a long timeframe.

In order to measure the activation of the UPR, FLAG tagged ATF-6 was transiently expressed in NRK cells. The cells were treated with tunicamycin, DTT, or DMSO for two hours, as well as the standard conditions for CPA-mediated luminal calcium depletion for 15 minutes in calcium-free medium with CPA and 15 minutes in calcium-free medium only. After that the cells were scraped and lysed. An enriched membrane fraction was generated using differential centrifugation. This fraction was then Western blotted for FLAG. Figure 32 shows that full-length FLAG-ATF-6 is expressed in all treatment groups. Because tunicamycin inhibits glycosylation in the ER, there are two separate bands of ATF-6 near 100 kD in that lane. As expected, both tunicamycin and DTT produced cleavage products of ATF-6 near 60 kD. CPA and DMSO, a negative control, both produced an extremely faint band of cleaved protein. Figure 32 shows the same lanes blotted for the ER resident protein calnexin. This Western blot confirms that equivalent amounts of endogenous protein were loaded in each lane. These results confirm that the conditions used for calcium depletion do not result in activation of the ATF-6 branch of the UPR. While it is possible that prolonged treatment induces an ER stress response, 30 minutes are not enough to induce UPR activation. Thus the trafficking effects that were observed with CPA are likely a result of calcium interacting directly with the fusion machinery and not the product of UPR signaling.

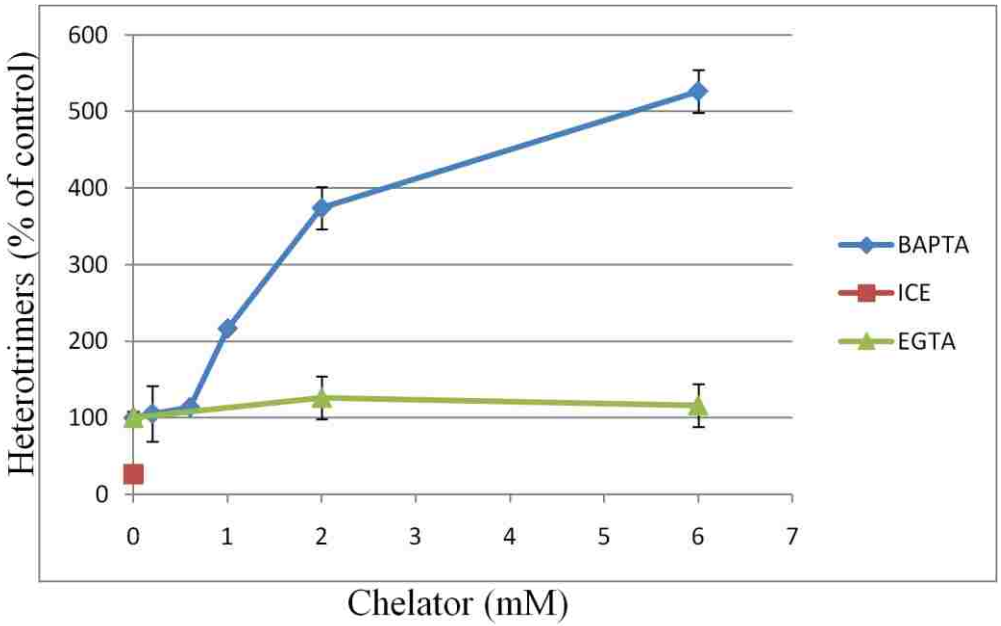

Figure 6 – BAPTA enhances COPII vesicle fusion *in vitro*.

COPII vesicle fusion was measured by heterotrimerization as described in Materials and Methods. Prior to 1 h fusion reactions, BAPTA or EGTA was added on ice for 20 minutes. Heterotrimers are expressed as a percentage of the 0 mM chelator reaction. Assay data are presented as means of duplicate determinations with error bars representing SE where larger than symbol size.

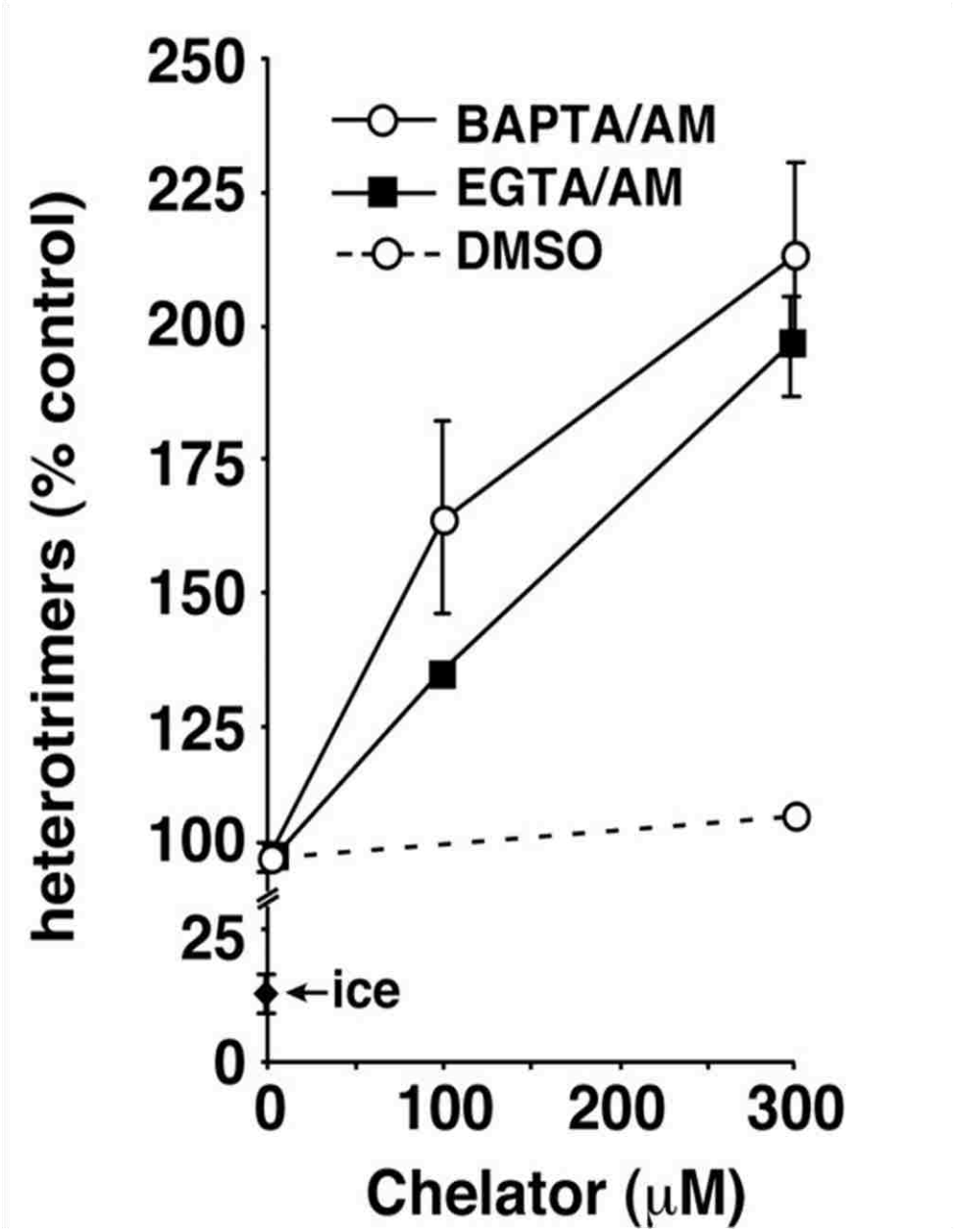

Figure 7 – Membrane permeant EGTA and BAPTA enhance homotypic COPII vesicle fusion

Effects of aminomethoxy (/AM) derivatives of BAPTA and EGTA on homotypic COPII vesicle fusion. Assay data are presented as means of duplicate determinations with error bars representing SE where larger than symbol size. This experiment was performed by Deb Nycz. Preliminary work for this experiment was carried out by Ashwini Joglekar (University of Michigan) and by myself.

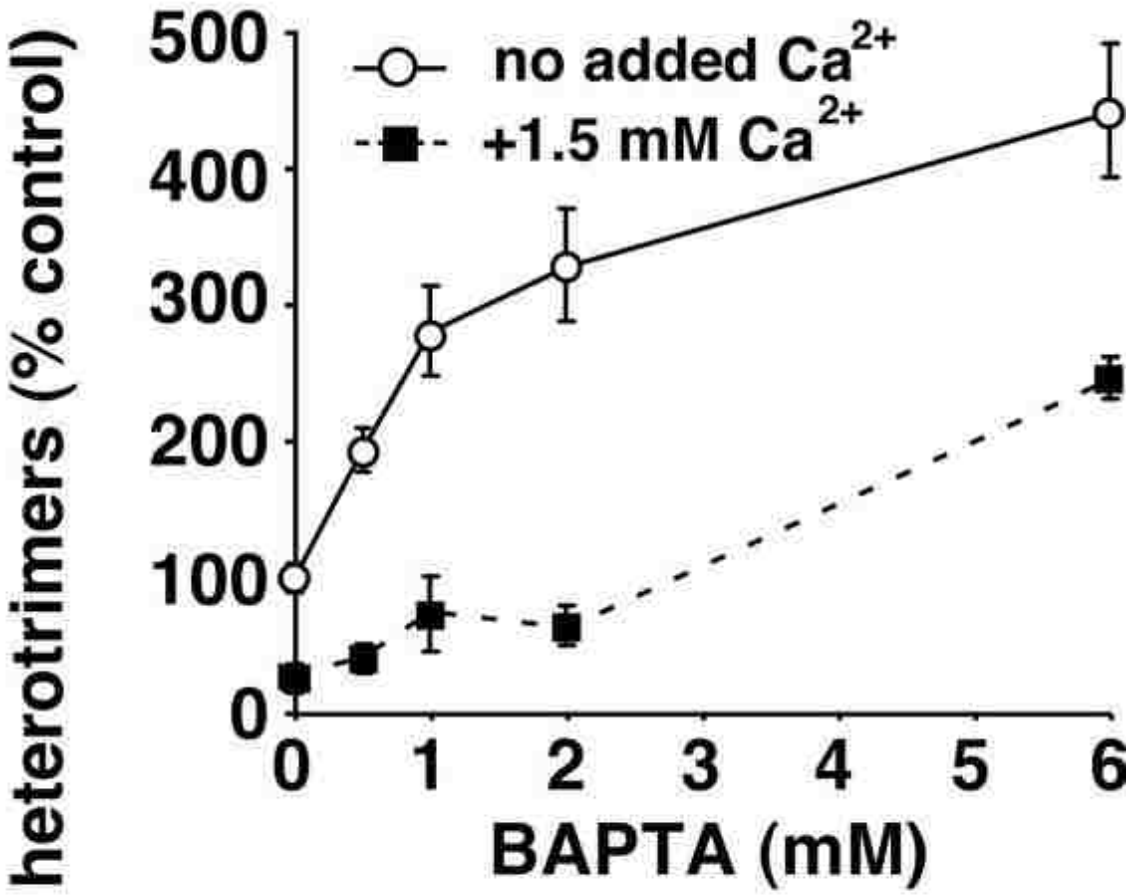

Figure 8 – Additional calcium increases the amount of BAPTA required for stimulation of homotypic COPII vesicle fusion.

COPII vesicle fusion was measured as described in Materials and Methods. The white circles show standard assay conditions with 0.18 mM calcium in the buffer. The black squares represent the addition of 1.5 mM calcium to the buffer. 0.5 mM EGTA is present throughout the assay.

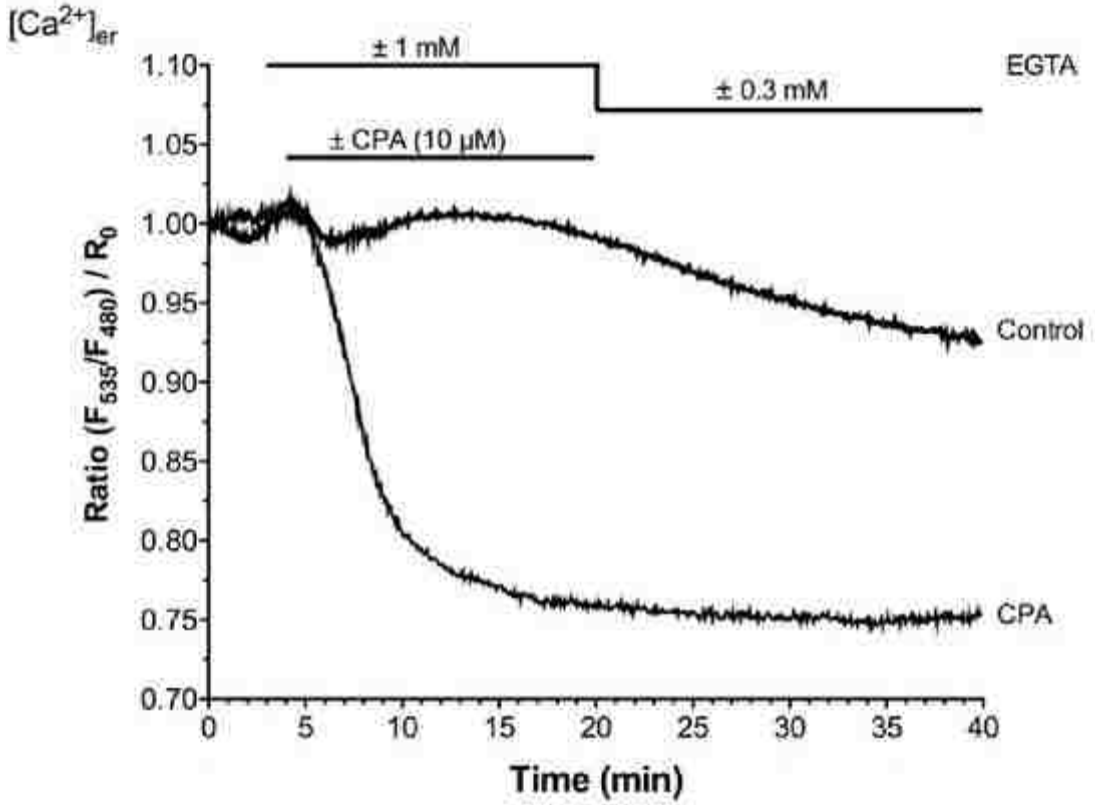

Figure 9 – CPA treatment results in decreased luminal calcium.

NRK cells were transiently transfected with the ER calcium sensor D1ER (Palmer et al., 2004). Foerster energy resonance transfer of the probe was measured. This experiment was performed by Ismene Fertschai, Roland Malli, and Wolfgang Graier.

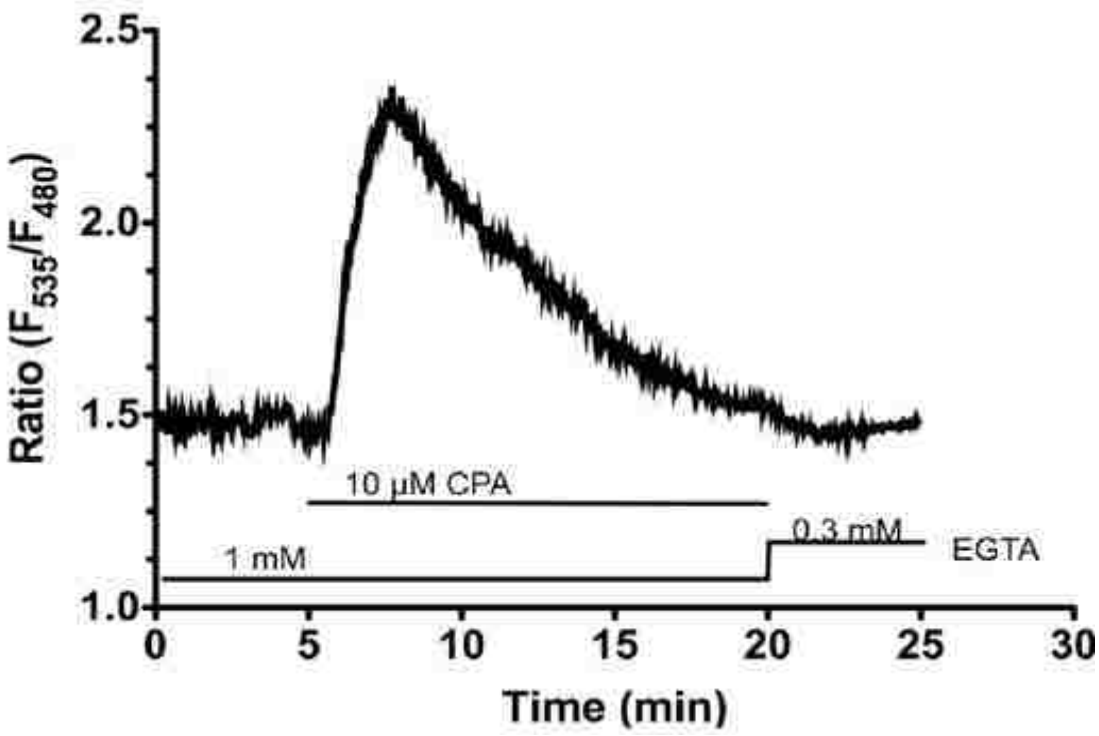

Figure 10 – Cytosolic calcium returns to normal levels after 15 minutes of CPA treatment.

NRK cells were transiently transfected with the ER calcium sensors YC3.6 and YC2.1 (Miyawaki et al., 1997; Nagai et al., 2004). Foerster energy resonance transfer of the probes was measured. This experiment was performed by Ismene Fertschai, Roland Malli, and Wolfgang Graier.

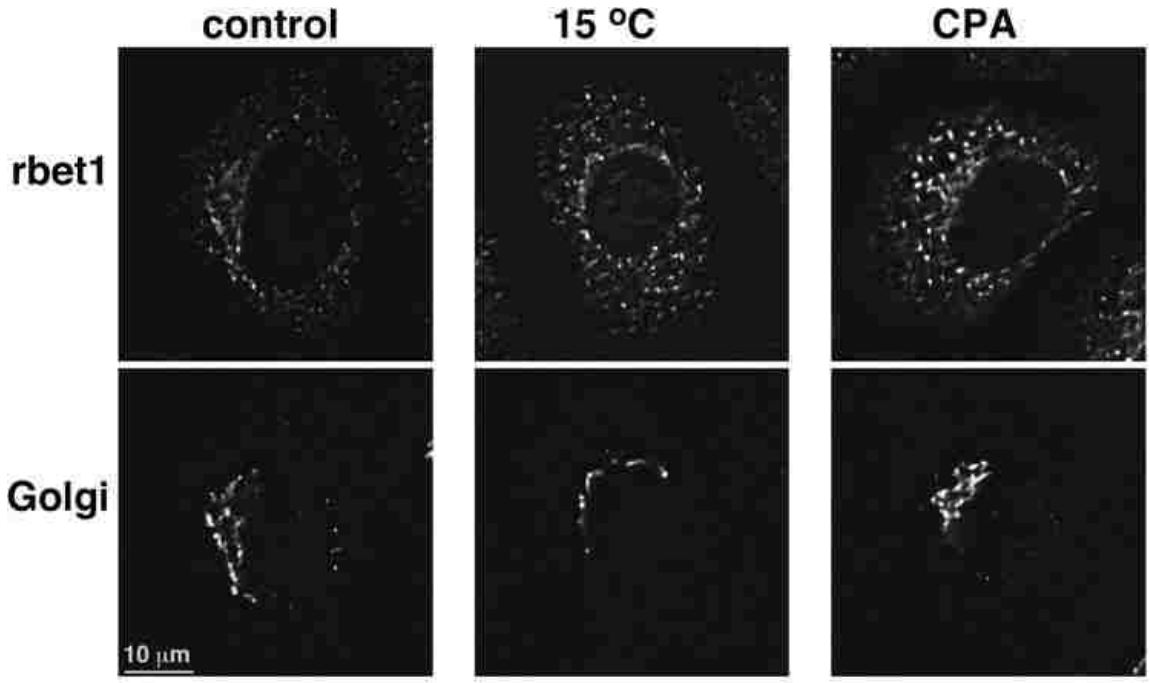

Figure 11 – Calcium depletion and 15°C treatment results in dramatic enlargement of ERGIC structures.

NRK cells were either mock-treated, incubated at 15°C for 30 minutes, or treated with CPA to deplete luminal calcium 15 minutes followed by 15 minutes in calcium-free medium. The cells were then fixed and immunostained for rbet1 and the Golgi marker GM130. Shown are single focal planes from deconvolved widefield image stacks.

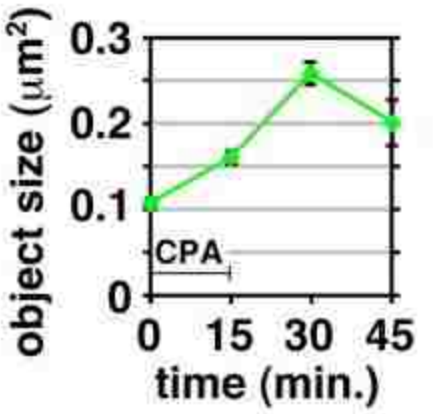

Figure 12 – Average rbet1 object size increases during luminal calcium depletion.

Cells were treated with CPA for 15 minutes followed by incubation in calcium-free medium. Peripheral rbet1 objects that were not associated with the Golgi were identified and measured by thresholding (see methods). Values represent average object size for cell of objects derived from at least 20 randomly chosen cells. Error bars display standard error.

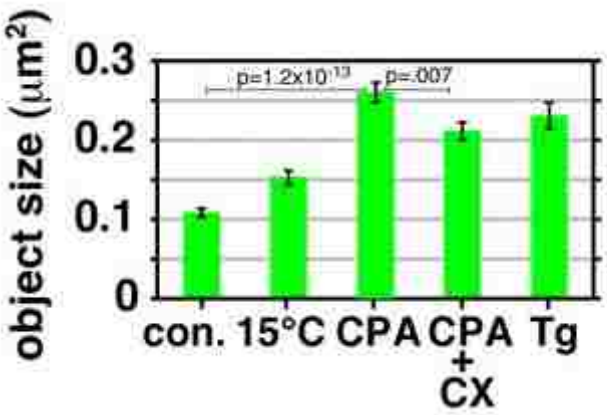

Figure 13—Average rbet1 object size increases with different calcium depleting drugs and is not dependent on new rbet1 synthesis.

15°C cells were incubated at that temperature for 30 minutes. CPA cells were treated for 15 minutes with CPA and incubated for 15 minutes in calcium-free medium. CPA + CX cells were treated for 15 minutes with CPA and incubated for 15 minutes in calcium-free medium, all in the presence of cycloheximide. Tg cells were treated for 30 minutes with thapsigargin in the presence of calcium free medium. Values represent per cell means derived from at least 20 randomly chosen cells. Error bars display standard error. Selected p values from two-tailed Student's *t* test are included.

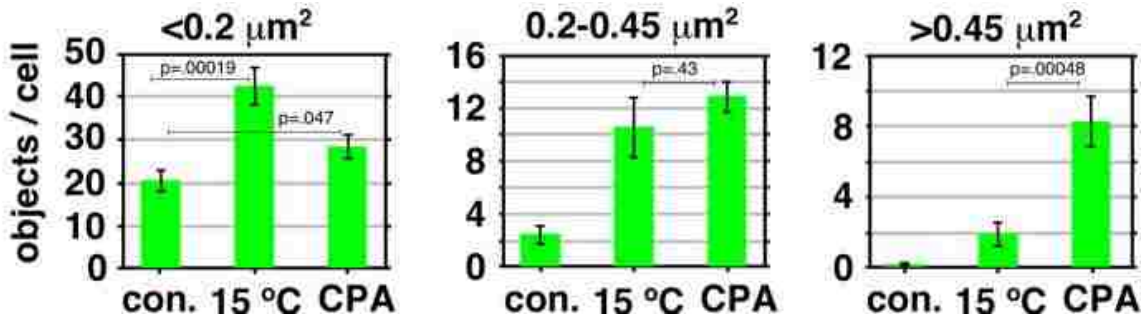

Figure 14 –Luminal calcium and 15°C treatment result in distinct changes in rbet1 distribution.

Quantification of peripheral rbet1 objects in experiments such as those described in Figure 12. Values represent per cell means derived from at least 20 randomly chosen cells. Error bars display SE. Only objects that fall within the size bins indicated above each plot are included in each panel. Selected p values from two tailed Student's *t* test are included. Areas of objects were calculated assuming that one image pixel width calibrates to 224 nm in the cell. Single-pixel objects are below resolution but were not eliminated from the size analysis; they did not contribute to the 0.2-0.45 μm^2 and >0.45 μm^2 size bins.

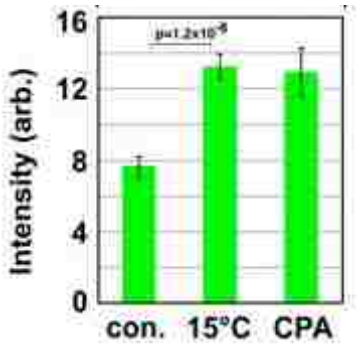

Figure 15 – Total rbet1 immunofluorescence increases upon depletion of luminal calcium as well as incubation at 15°C.

Cells were stained with monoclonal rbet1 antibody. An ROI was drawn around the whole cell of one deconvolved focal plane. Total rbet1 (16G6 antibody) immunofluorescence was measured. Values represent per cell means derived from at least 20 randomly chosen cells. Error bars display standard error. p value from two-tailed Student's *t* test is included.

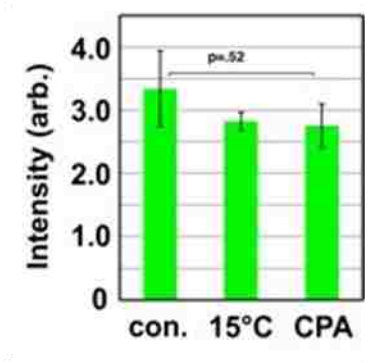

Figure 16 – Total rbet1 expression does not change significantly upon depletion of luminal calcium or incubation at 15°C.

Cells were lysed and equal amounts of protein were analyzed by SDS-PAGE electrophoresis and Western blotting with a monoclonal rbet1 antibody (see Methods). Values represent per means derived from at least two separate experiments. Error bars display standard error. p value from two-tailed Student's *t* test is included.

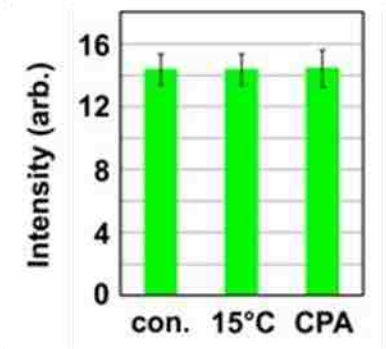

Figure 17 – Total GM130 immunofluorescence remains constant during depletion of luminal calcium as well as incubation at 15°C.

Cells were stained with GM130 antibody. An ROI was drawn around the whole cell of one deconvolved focal plane. Total GM130 immunofluorescence was measure. Values represent per cell means derived from at least 20 randomly chosen cells. Error bars display standard error.

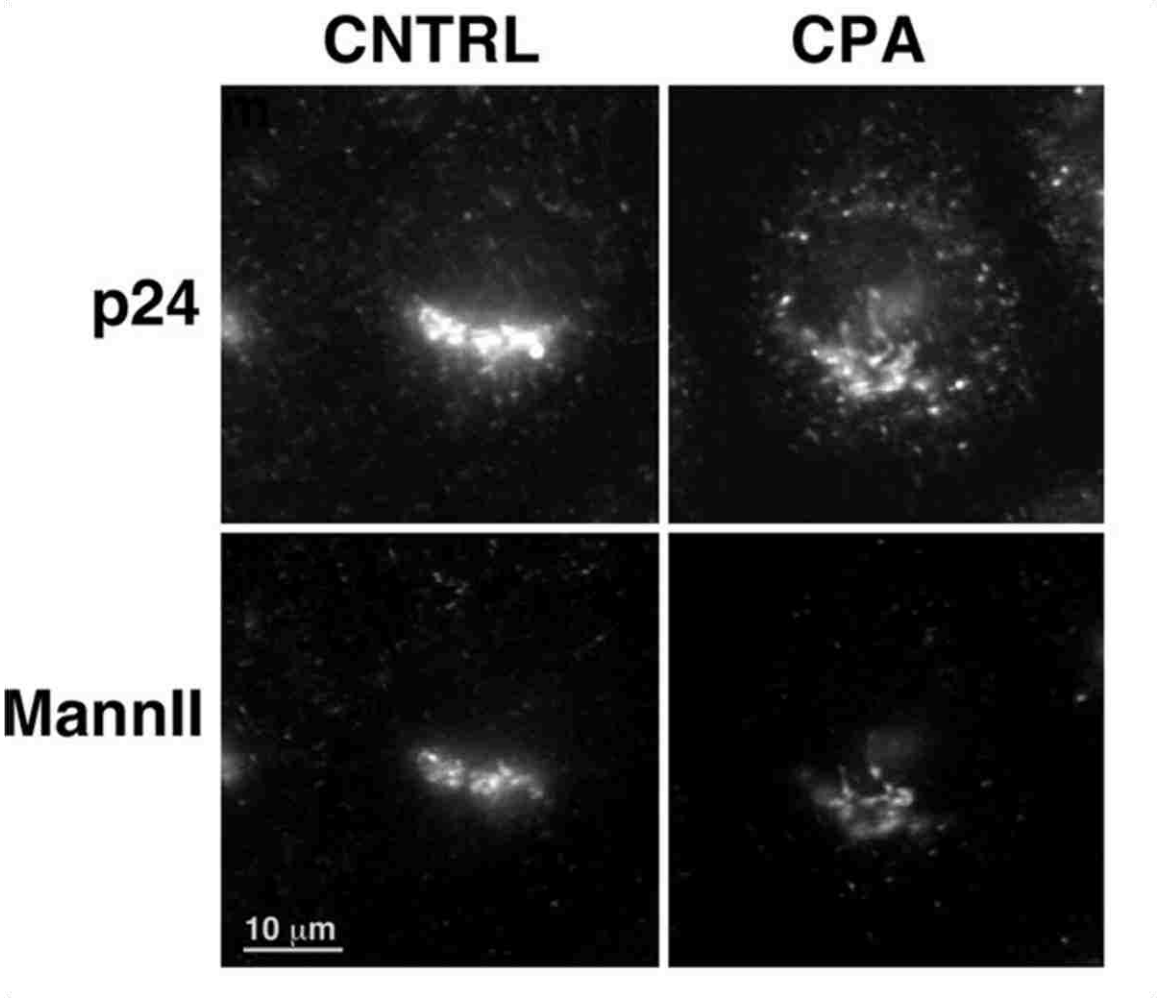

Figure 18 – Luminal calcium depletion results in the enlargement of p24-positive ERGIC structures.

NRK cells were either mock-treated or treated with CPA to deplete luminal calcium, then fixed and immunostained for p24 and the Golgi marker mannosidase II. Shown are single focal planes from deconvolved widefield image stacks.

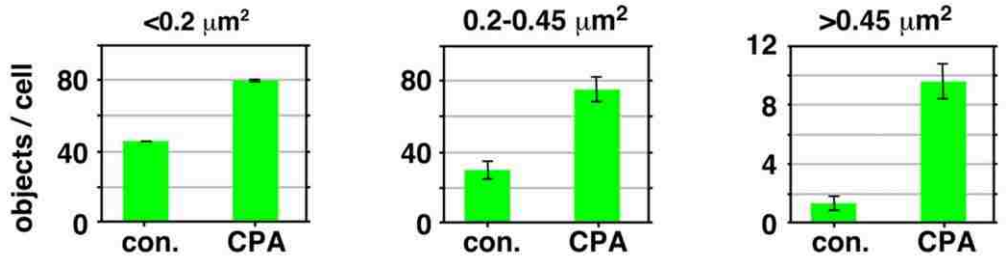

Figure 19 –Luminal calcium depletion results in the production of p24 positive ERGIC structures of different sizes.

Quantification of peripheral objects positive for p24. Objects were organized in three size bins under the same experimental conditions as for Figure 15. Values represent per cell means derived from at least 20 randomly chosen cells. Error bars display standard error.

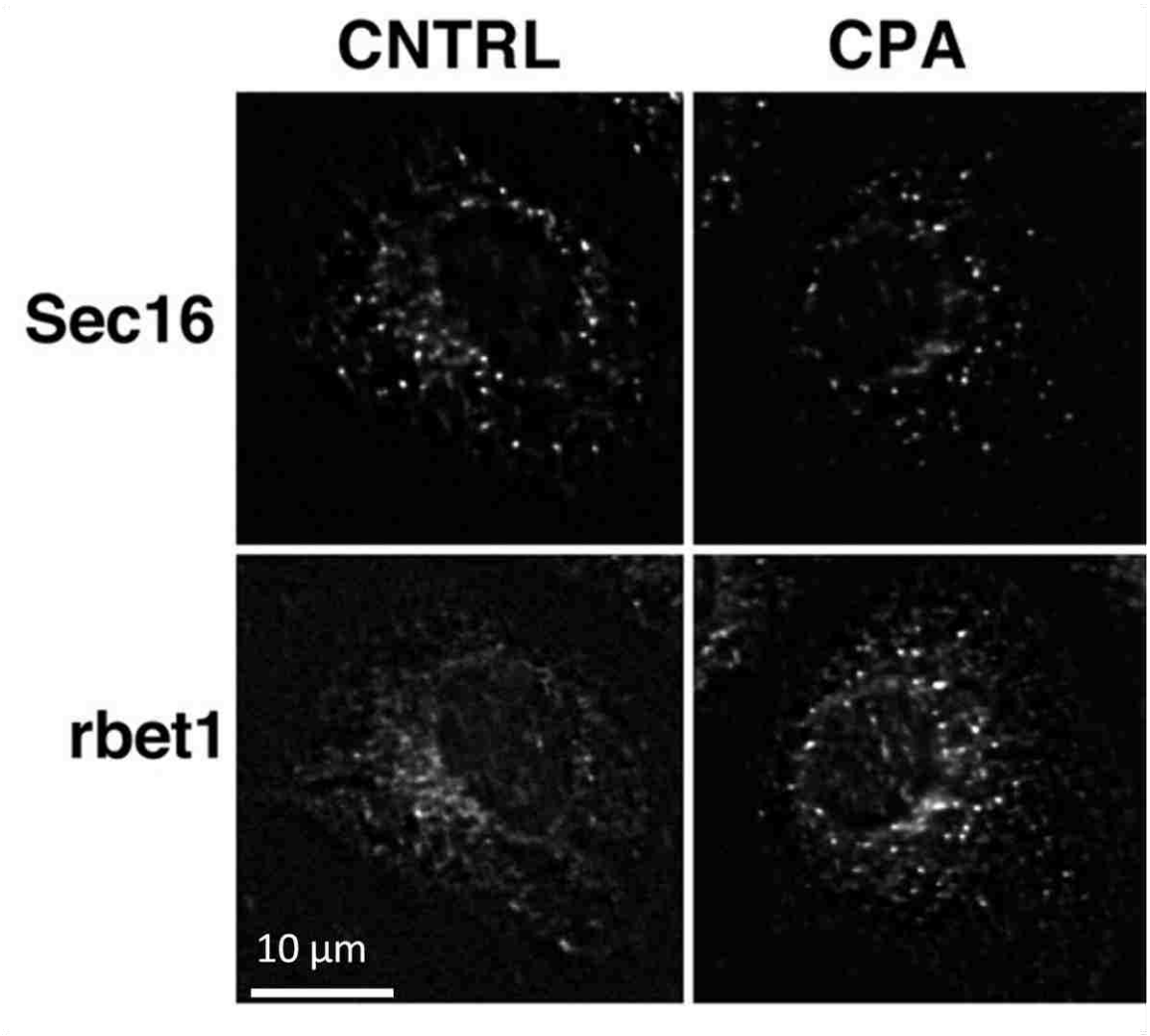

Figure 20 – Sec16 ERES staining remains unchanged following luminal calcium depletion.

Immunolabeling for rbet1 and Sec16 was performed using the same experimental conditions as described in Figure 19.

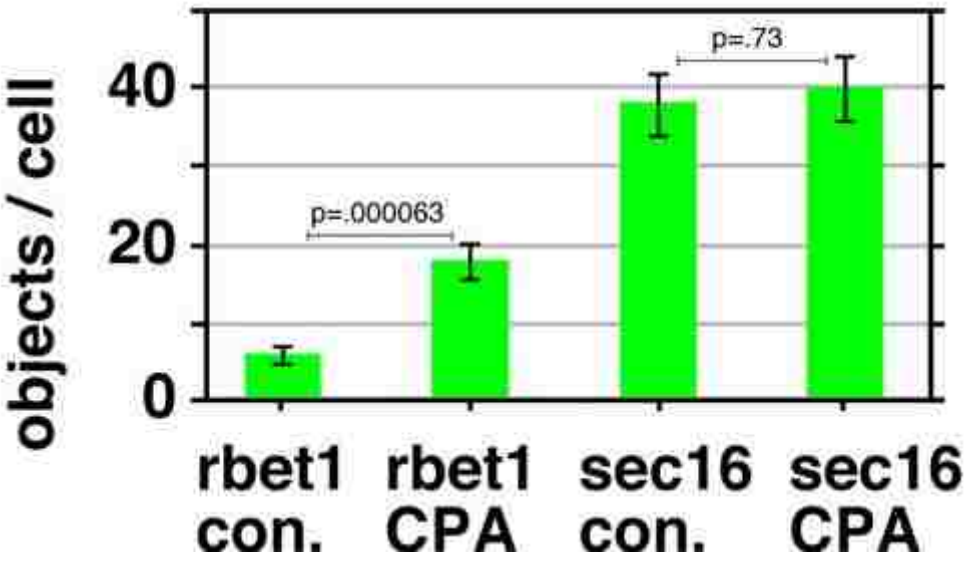

Figure 21 – Sec16 peripheral object abundance remains unchanged in cells depleted of luminal calcium.

Quantification of rbet1 and Sec16 labeling from Figure 21. All size bins were included in one analysis. The rbet1 and Sec16 object data are from exactly the same set of double-labeled NRK cells. Values represent means derived from at least 20 randomly chosen cells. Error bars display SE. Selected p values from two-tailed Student's *t* test are included.

co-staining	v. large peripheral objects (>90%tile) positive for rbet1	v. large peripheral objects (>90 %tile) positive for rbet1 also positive for COPI or ERES	% positive for both
rbet1 vs. sec16	58	57	98.28
rbet1 vs. β-COP	67	49	73.13

Table 1 – Co-localization of large peripheral objects.

The five largest peripheral rbet1 structures in each cell were analyzed for this table. For each of these, co-staining for Sec16 and beta-COP was scored by generating a separate mask that was also thresholded at four times the cellular background. Any overlap between the rbet1 mask and the Sec16 or beta-COP mask was counted as co-localization.

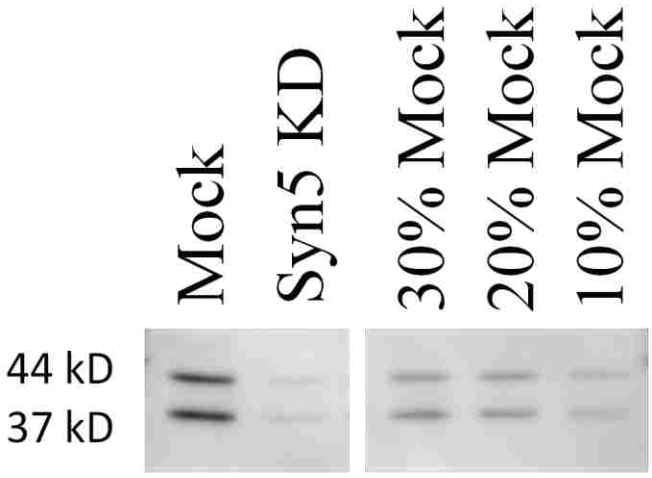

Figure 22 – Syntaxin 5 is knocked down more than 90% in NRK cells.

Western blot of cell lysates. The lanes labeled “mock” and “Syn5 KD” had equal amounts of protein loaded. The remaining lanes each had a percentage of mock loaded. Both expected Syntaxin 5 isoforms at 44 kD and 36.6 kD are knocked down better than 90%.

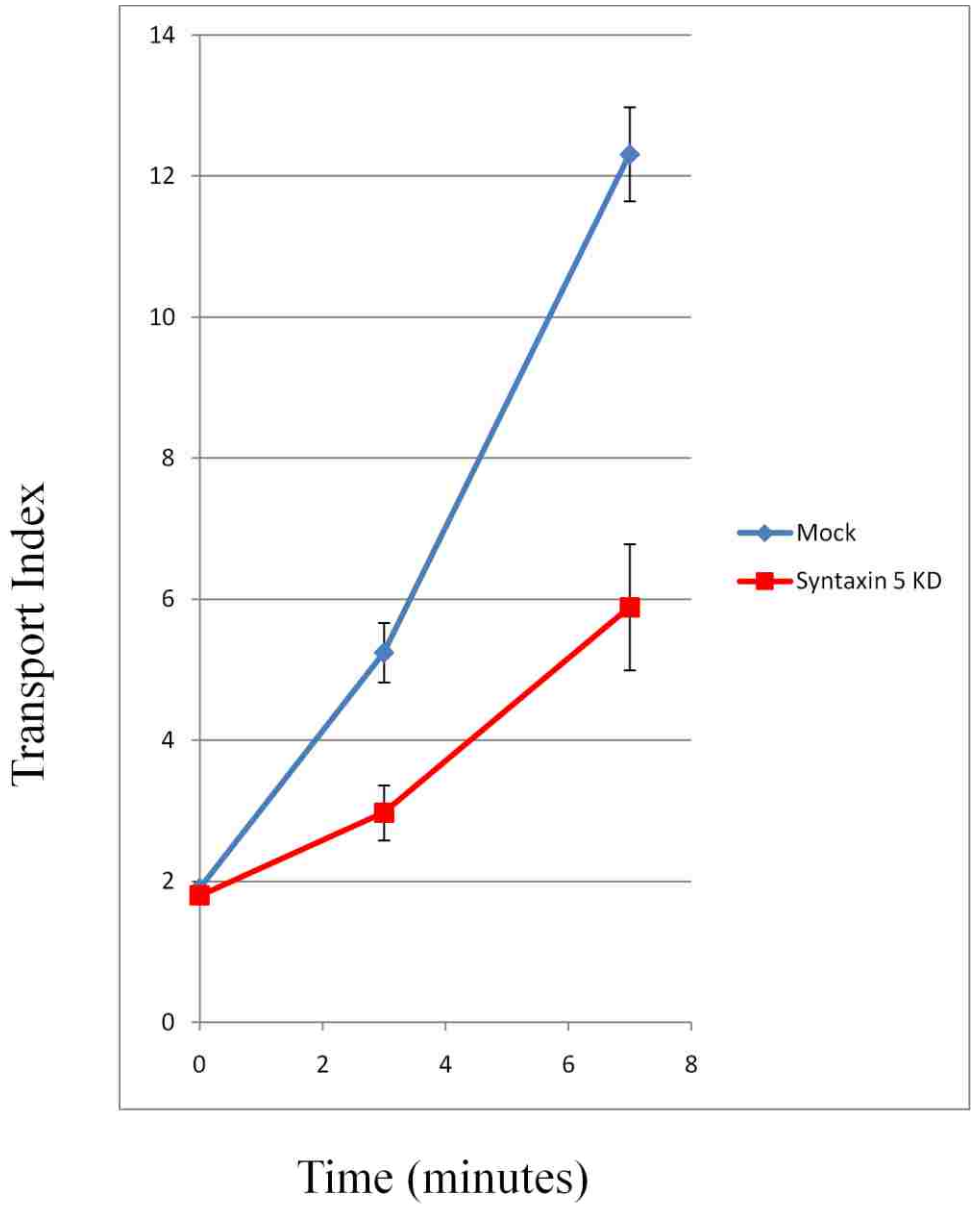

Figure 23 – VSV-G-GFP trafficking impairment due to Syntaxin 5 knockdown is measurable using the transport index ratio.

Cells were mock-treated or treated with Syntaxin 5 siRNA. After transfection with VSV-G-GFP, the cargo was synchronized by incubating the cells at 10°C. Cargo was released by shifting the cells to 32°C. Arrival of VSV-G-GFP in the Golgi was then measured by fluorescence and quantified as described in the methods. Values represent means derived from at least 20 randomly chosen cells. Error bars display SE.

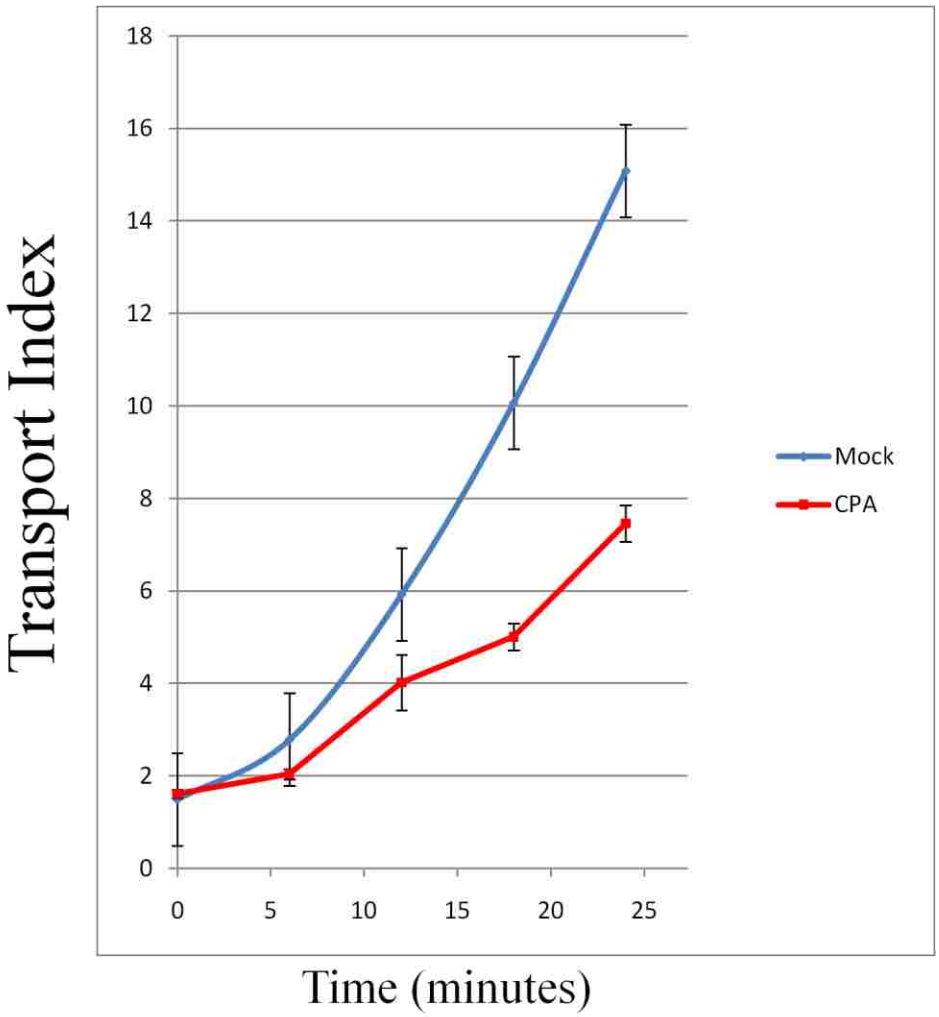

Figure 24 – Depletion of luminal calcium decreases ER to Golgi transport of VSV-G-GFP.

VSV-G-GFP expressing cells were CPA treated at 40°C. Cargo was then released by shifting the cells to 32°C. Arrival of VSV-G-GFP in the Golgi was measured as described in the methods. Values represent means derived from at least 20 randomly chosen cells. Error bars display SE.

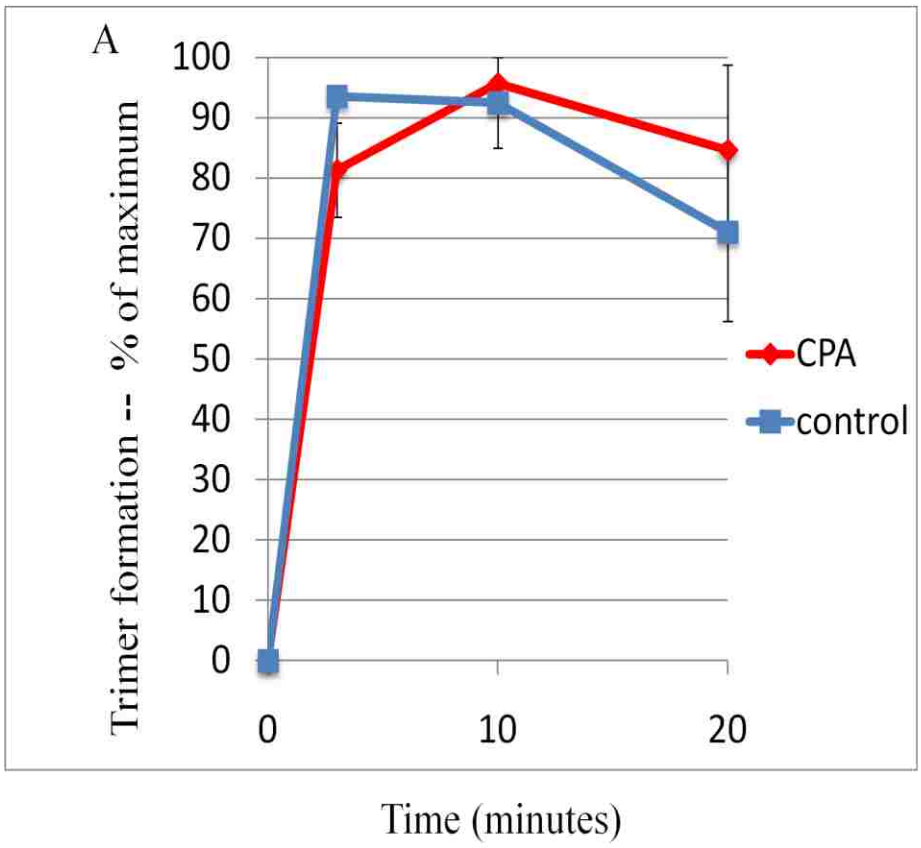

Figure 25 – VSV-G trimerizes maximally in three minutes.

Cells expressing VSV-G-myc or VSV-G-GFP were kept at 40°C. Following control or CPA treatment VSV-G was released from the ER at 32°C. Cells were lysed and VSV-G trimer antibody I14 was used for immunoprecipitation of assembled trimers. (A) Immunoprecipitated trimers were quantified by Western blot with anti-myc or anti-GFP antibody. The graph was generated using three independent experiments. Error bars display the standard error of the mean. To prepare the graph the 0 minute value was subtracted from each data point. Then each data point was expressed as a percentage of the maximum value. (B) Example Western blot showing immunoprecipitated VSV-G trimers.

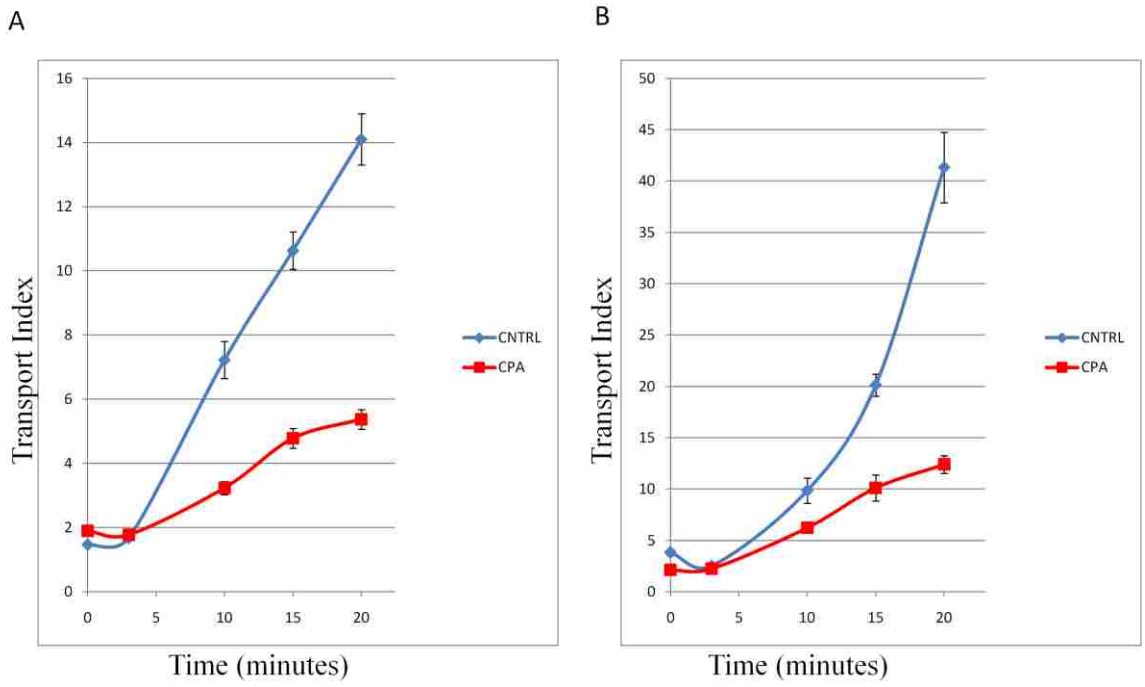

Figure 26 – VSV-G-GFP trimers are transported more slowly to the Golgi apparatus following luminal calcium depletion.

VSV-G-GFP expressing cells were CPA-treated at 40°C. Cargo was then released by shifting the cells to 32°C. Cells were fixed and stained for VSV-G trimers using the I-14 antibody. Arrival of total VSV-G-GFP (A) or VSV-G trimers (B) was measured by immunofluorescence as described in the methods. Cycloheximide was present during the 32°C incubations. Values represent means derived from at least 20 randomly chosen cells. Error bars display SE.

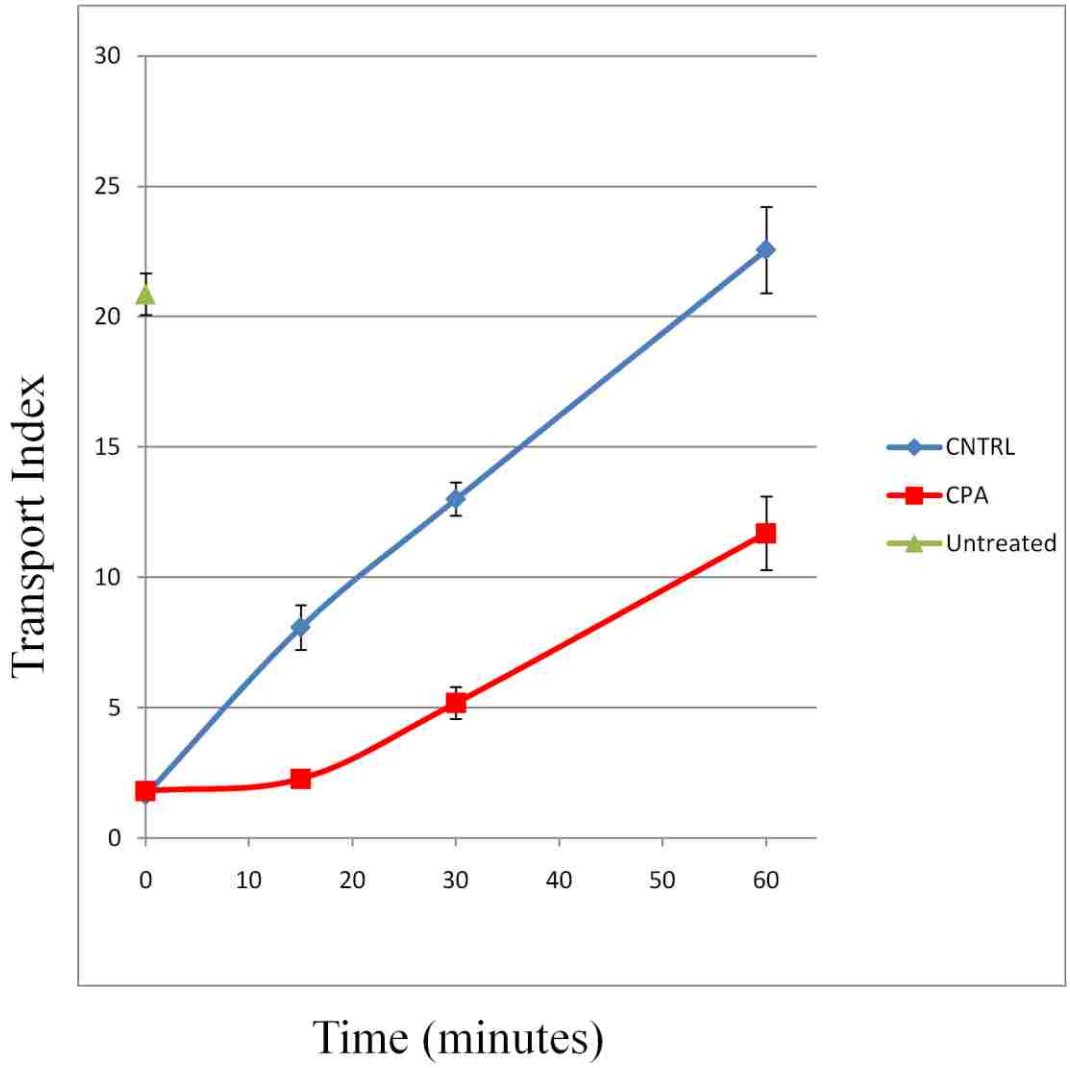

Figure 27 – Golgi recovery after brefeldin A washout is impaired in cells depleted of luminal calcium.

Golgis were dispersed using brefeldin A (BFA) for 45 minutes. For calcium depletion, the usual CPA conditions were employed for the final 15 minutes of the BFA incubation. After the BFA washout (t = 0 on plot), CPA-treated cells were allowed to recover in calcium-free medium whereas control cells recovered in normal medium. Untreated cells were grown in normal medium. Cells were fixed and stained for Mannosidase II. Cycloheximide was present in the medium throughout the experiment. Values represent means derived from at least 20 randomly chosen cells. Error bars display SE. This type of experiment was first performed by Ting Wang.

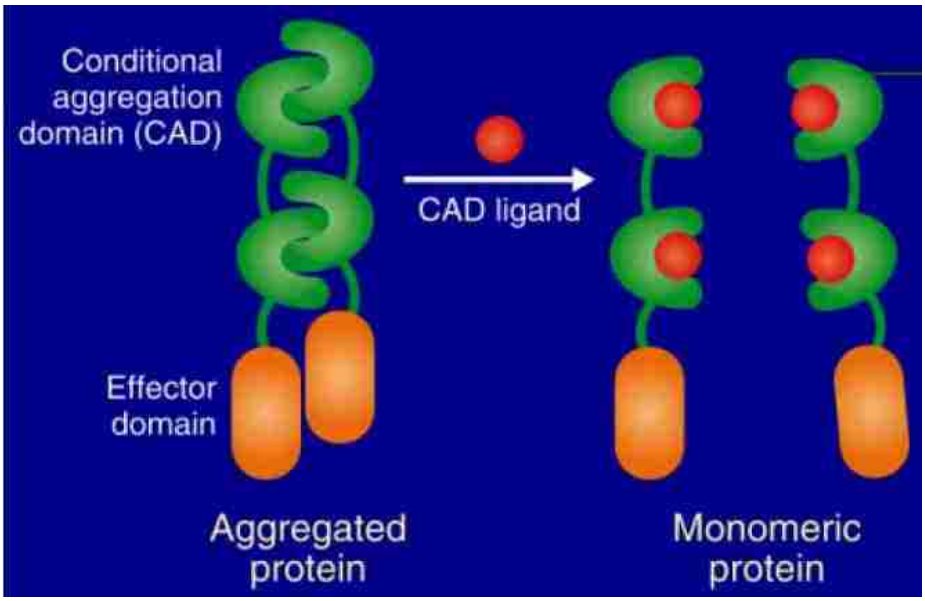

Figure 28 – Graphical representation of the conditional aggregation domain.

A fusion protein containing a signal sequence, eGFP, and the aggregation domain was constructed and has been described previously (Gordon et al., 2010). This construct was expressed stably in HeLa cells. Cells build up cargo in the ER which cannot be exported due to the aggregates that they form. Addition of the drug AP21998 frees the conditional aggregation domains and allows the protein to leave the ER.

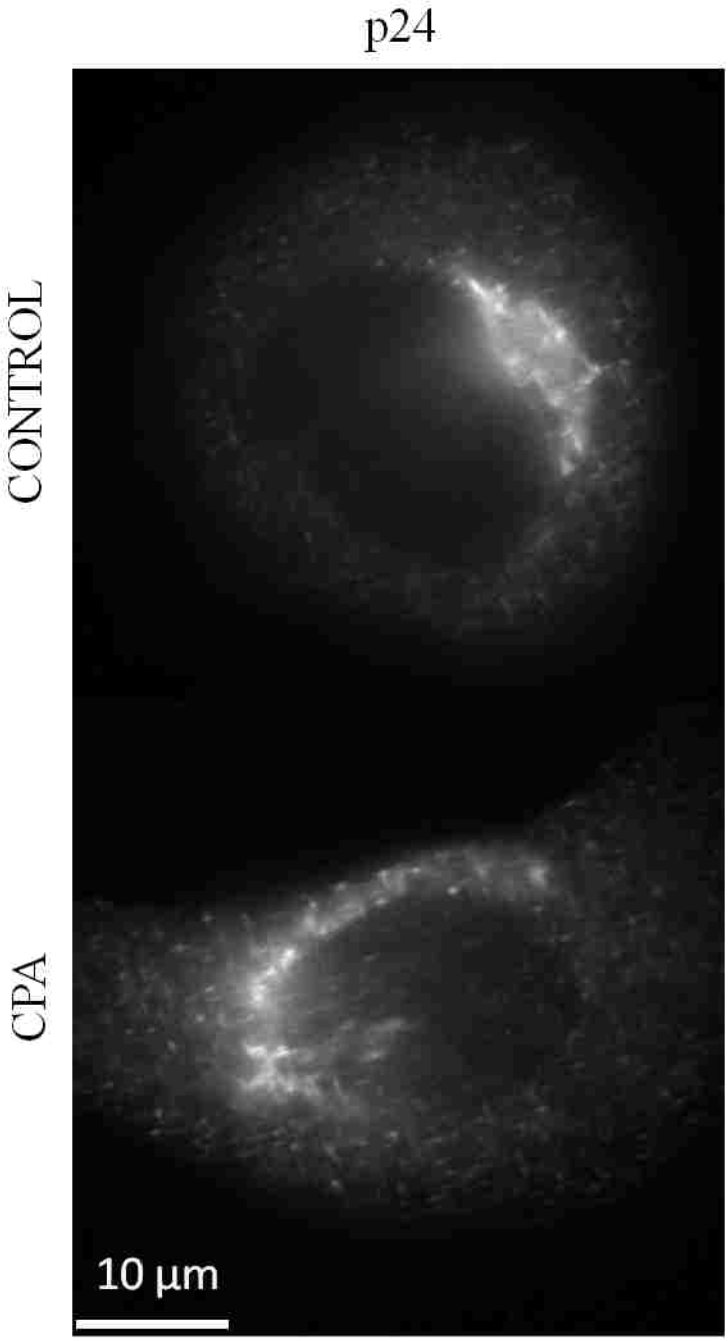

Figure 29– Calcium depletion in HeLa cells results in an increase of large peripheral p24 structures.

HeLa cells were either mock-treated or treated with CPA to deplete luminal calcium, then fixed and immunostained for p24.

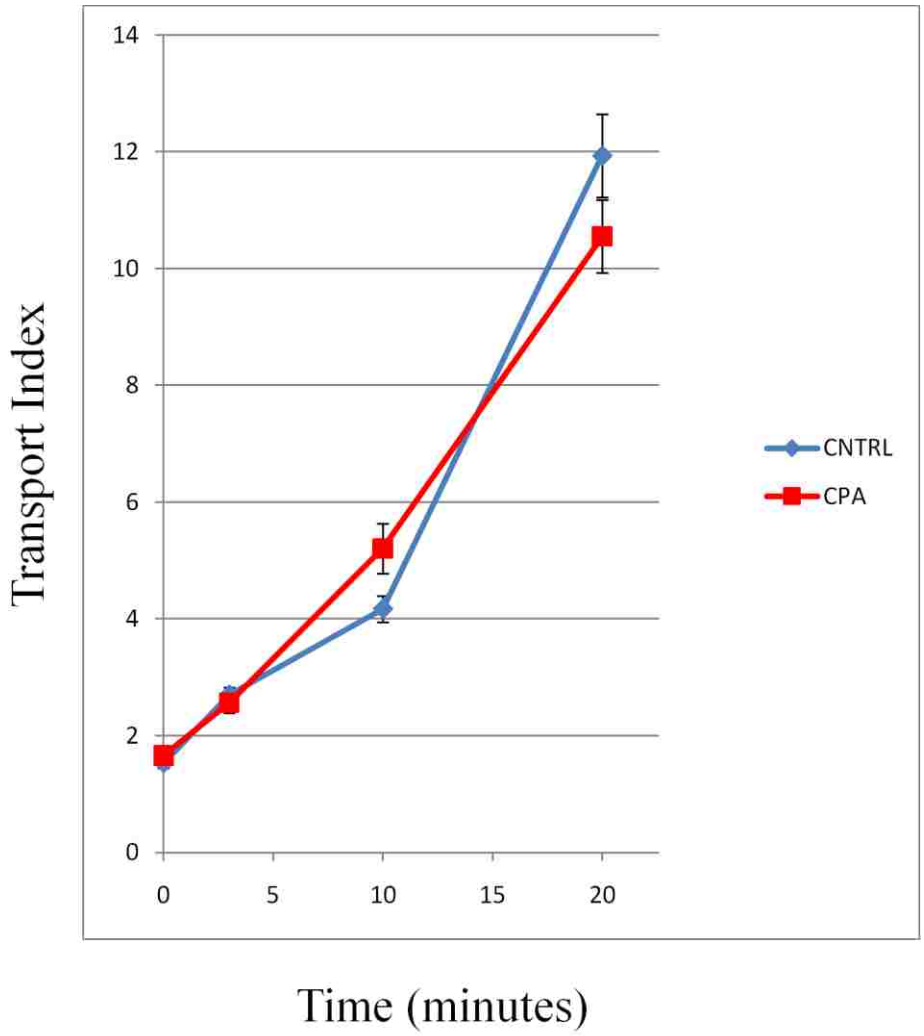

Figure 30 – Bulk cargo transport is not affected by the depletion of luminal calcium

HeLa cells stably expressing GFP fused to a conditional aggregation domain were calcium depleted as described above. After calcium depletion cargo aggregation was reversed by the addition of the drug AP21998. Mean ER intensity and maximum Golgi intensity for GFP were then measured and the transport index was generated as described above. Cycloheximide was added to the medium at the same time as AP21998. Values represent means derived from at least 20 randomly chosen cells. Error bars display SE.

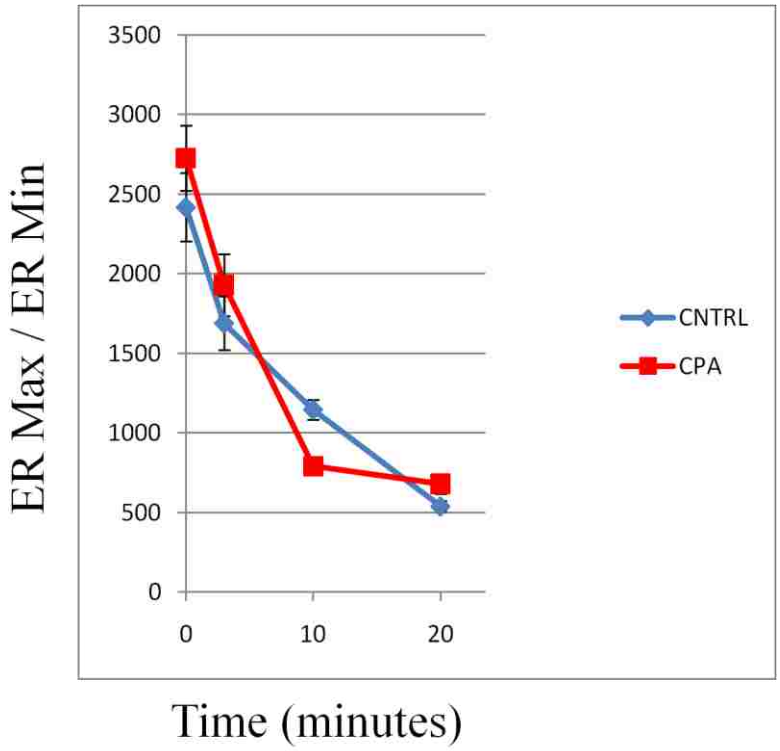

Figure 31 – Cargo de-aggregation occurs at a rapid rate for control and CPA treated cells.

The ER intensities of GFP for cells quantified in Figure 31 were measured. For each cell a maximum ER and a minimum ER intensity were measured. Values represent mean ratios derived from the same cells as measured in Figure 31. Error bars display SE.

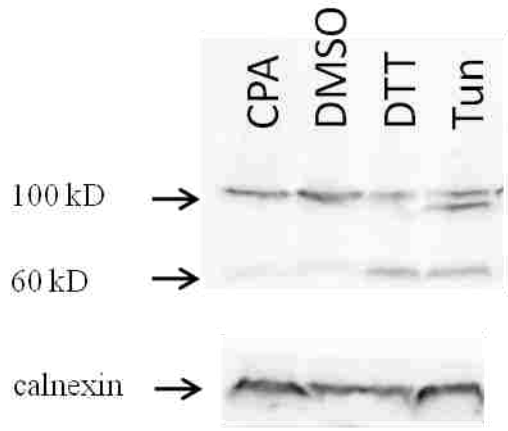

Figure 32 – ATF-6 is not activated by typical conditions for luminal calcium depletion.

NRK cells were transfected with FLAG-ATF-6. Lane 1: cells were treated with CPA for 15 minutes followed by 15 minutes in calcium free medium as described above. Lane 2: Cells were incubated in 0.5% DMSO for 2 hours. Lane 3: 1 mM dithiothreitol (DTT) was added to cells for 2 hours. Lane 4: 2 µg/mL tunicamycin (Tun) was added to cells for 2 hours. Cells were lysed and an enriched membrane fraction was generated. This was analyzed by SDS-PAGE electrophoresis followed by Western blotting for FLAG. Uncleaved ATF-6 is visible at 100 kD, whereas the cleaved ATF-6 product is visible at around 60 kD as expected. A Western blot for calnexin confirms that comparable amounts of endogenous protein were loaded in each lane.

Discussion

Major contributions of this thesis to the field

The driving hypothesis for the work presented here is that luminal calcium acts as a regulator of membrane trafficking from the ER to the Golgi apparatus. In these experiments, I have for the first time described several such roles for luminal calcium. Previous work used blunt manipulations to cells, for example using chelation of all cellular calcium using BAPTA/AM and EGTA/AM and low resolution assays that did not allow discrete analysis of particular trafficking steps (Chen et al., 2002). The major contributions that arise out of my work are the following:

1) In cell free *in vitro* experiments, luminal calcium suppresses the fusogenicity of COPII vesicles. This result implies that calcium acts on the outside of the vesicle through a calcium sensor that interacts with the fusion machinery. This inhibition of the fusion machinery exerted by calcium may function as a way to target vesicles to fuse with the correct target compartment after they reach maturity and move away from the ERES. Other work from the Hay laboratory has indentified the likely calcium sensor Apoptosis Linked Gene 2 (ALG-2). This protein is a penta-EF hand calcium sensing protein which interacts with the COPII subunit Sec31 and may be the sensor that interacts with leaking luminal calcium (Bentley et al., 2010).
2) Luminal calcium regulates the morphology of the ER to Golgi intermediate compartment. Specific inhibition of SERCA ATPases results in a dramatic expansion of the ERGIC and a concentration of recycling proteins in the

intermediate compartment. These morphological changes suggest changes in the trafficking patterns between the ER and the Golgi apparatus. This change is also distinct from the incubation of cells at 15°C, a manipulation commonly used to trap cargo in the ERGIC, which implies it involves a distinct mechanism. The development of this luminal calcium depletion should be an important tool for studying further aspects of the intermediate compartment.

3) Luminal calcium is required for optimal ER to Golgi trafficking of membrane proteins. Specific luminal calcium depletion causes slowed ER to Golgi transport of VSV-G and mannosidase II. These results show that the morphological changes of the ERGIC caused by depletion of luminal calcium affect cargo trafficking. It is unclear whether these trafficking defects are a direct result of COPII vesicle fusogenicity changes (as observed during *in vitro* experiments in part 1) or whether other models could better explain the results as discussed below.

Luminal calcium suppresses COPII vesicle fusion *in vitro*

A surprising result from this study is that calcium suppresses *in vitro* membrane fusion of COPII vesicles. This is effect of calcium is opposite to other membrane fusion events including regulated exocytosis, endosomes fusion, and intra Golgi transport (Burgoyne and Clague, 2003). In those cases calcium provides a stimulus that triggers membrane fusion, or a basal amount of calcium is required to proceed with membrane fusion. It is possible that the unique calcium gradients in the very early secretory pathway provide an ideal opportunity for calcium to play a different regulatory role. The

high calcium concentration in the ER, followed by low calcium concentrations in the ERGIC could be utilized as a measure of compartmental maturity.

ER free calcium is usually very high and is maintained by SERCA pumps in the membrane. It is possible that, because SERCA pumps are not loaded onto COPII vesicles, a nonspecific calcium leak causes free luminal calcium in the secretory pathway to progressively decrease as vesicles mature. Thus, the ever-changing calcium signature of ERGIC structures could be used in a manner not yet appreciated at other transport steps. Vesicles that are loaded with high luminal calcium when they bud from the ER could be leaking calcium as they mature. Early after vesicle budding the leaking calcium could act as a signal preventing fusion of the vesicle back with the donor compartment or with other immature transport vesicles. This would be a signal independent of the protein machinery, which is present on both the donor compartment and the newly formed vesicle. Simultaneously, the leaking calcium signal could act as a way of triggering preferential fusion of the COPII vesicle with target compartments that exhibit a lower calcium signature. These would be mature ERGIC structures that are going to be trafficked towards the Golgi apparatus. This signal would presumably act as a temporal regulator of the ERGIC lifecycle. While the calcium will act early on after the vesicle is budded, the signal will be lost when the luminal calcium expires. Any molecules that act in a calcium-dependent way on the outside of the vesicle will dissociate when the calcium levels inside the vesicles are too low to generate a signal to the outside of the vesicle.

Additionally, in the absence of an already existing ERGIC structure, COPII vesicles could eventually be triggered to form nascent ERGIC structures by undergoing several steps of homotypic fusion after losing sufficient calcium. This represents a

mechanism to dictate the biogenesis of nascent transport compartments when the existing ERGIC compartments are absent. It is possible that mature ERGIC structures have lost their calcium gradient by the time they reach the Golgi apparatus. At the Golgi, Golgi calcium ATPases are responsible for maintaining a high calcium concentration inside the Golgi cisternae (Wuytack et al., 2002). Hence, the previously shown requirement for the fusion of pre-Golgi intermediates with the Golgi as well as the fusion within the Golgi would direct an ordered fusion of mature ERGIC structures with the appropriate, calcium rich target compartment (Beckers and Balch, 1989; Porat and Elazar, 2000). The calcium leak on the vesicle could maintain a calcium puff on the outside of the membrane (Figure 4). This calcium cloud could interact very locally with machinery near the leak on the outside of the vesicle. While it is possible for some amount of calcium ions to diffuse across the membrane, a sustained signal aimed at protein machinery attached to the membrane is likely linked to a specific leak channel. However, there are no known calcium channels that are loaded onto COPII vesicles. It is conceivable that small amounts of the ER calcium channels such as IP3Rs and RyRs are cycled through the ERGIC, but it is also possible that COPII vesicles contain a yet unidentified calcium leak channel. Future studies will have to clarify the identity of leak channels on these vesicles.

The mechanism by which BAPTA affects COPII vesicles is unclear. The functional selectivity of BAPTA over EGTA combined with the lack of difference between BAPTA/AM and EGTA/AM suggests that the calcium leaking from the lumen of the vesicle acts close to the site of membrane fusion. However, neither BAPTA/AM nor EGTA/AM chelation could generate the same level of fusion stimulation as BAPTA

lacking the aminomethoxy group. Hydrolysis of these aminomethoxy esters generates formaldehyde and acetic acid. The release of these could have non-specific suppressive effects on COPII vesicle fusion. Reproducing the increase of fusion *in vitro* using ionophores to release calcium has been unsuccessful (data not shown). This result suggests that the functionally important pool of calcium is resistant to such treatment. It is possible that this pool of calcium is bound on the outside of the vesicle near the membrane and that the hydrophobic rings on BAPTA allow this molecule to chelate close to the membrane, which EGTA cannot. BAPTA is also a uniquely high ionic strength molecule, yet hydrophobic with the potential for non-selective extraction of peripheral membrane proteins. Regardless what the exact mechanism of BAPTA activation is, it has lead to closer investigation of the role of luminal calcium in the early secretory pathway.

Luminal calcium regulates the distribution of intermediate compartment elements

Specific depletion of luminal calcium using SERCA pump inhibitors results in enlarged peripheral structures that contain ERGIC markers. However, it is unclear whether these structures are in fact larger ERGICs representing a fusion product of COPII vesicles. It is also possible that the enlarged structures are an accumulation of unfused COPII vesicles or just an increased amount of vesicle buds. Because of the resolution limits of standard light microscopy, it not possible to definitely say what exactly the large peripheral structures are. Electron microscopy studies will be necessary to determine the exact nature of these structures. It is also not clear that these structures are really increasing in size or whether they are just collecting more antibody labeling

under the staining conditions used. The total rbet1 staining increases in CPA-treated cells, which could point towards an increase of labeling of these structures rather than expansion (Figure 15). On the other hand, 15°C also caused a redistribution of rbet1 to the periphery without the appearance of large objects. This implies that the apparent enlargement of ERGIC elements during CPA treatment may in fact signify a bona fide morphological change.

It is also not clear what the mechanistic differences between CPA treatment and 15°C incubation are. At 15°C, microtubules may begin to de-polymerize. Therefore, intermediate structures might be trapped in the periphery, unable to transport to the Golgi apparatus. However, the CPA effect must not have merely stranded ERGIC in the periphery because the effects on size distribution indicate that the two treatments produce distinct kinds of ERGIC structures.

Luminal calcium is required for optimal ER to Golgi transport of membrane proteins

Depletion of luminal calcium results in dramatic changes in the structure of the ERGIC, severely impairs the trafficking of VSV-G to the Golgi apparatus, and decreases the speed of Golgi reformation after brefeldin A treatment (Figures 11, 24, 28). There might be some decrease in trafficking due to effects on protein folding, however, the best interpretation of the data is that the majority of the kinetic decrease in trafficking is caused by direct effects on the trafficking machinery. When looking only at the kinetics of already folded proteins, Golgi arrival of VSV-G is significantly impaired (Figure 27). While these experiments were designed to minimize the impact of folding effects caused by luminal calcium depletion the transport results still need to be interpreted cautiously.

All of the available kinetic assays that observe trafficking between the ER and the Golgi require cargo buildup in the ER and thus could in principle be affected by the status of ER folding chaperones. Because calcium plays such an important role in protein folding in the ER it is extremely hard to distinguish calcium effects on folding rather than trafficking.

While a previous study has claimed that UPR activation by thapsigargin causes kinetic defects in VSV-G trafficking, the experiments presented here show that the ATF-6 pathway is not activated in cells with depleted luminal calcium using the CPA conditions I developed (Figure 31) (Amodio et al., 2009). Amodio et al., 2009 discovered that activation of the UPR results in a decrease of ER to Golgi trafficking kinetics as well as an accumulation of small ERGIC-53 positive vesicles. However, their protocols would result in sustained high cytosolic calcium that complicates the interpretation of their data and comparison to my results. ER stress also directly results in the transcription of the COPII subunit Sec23 in order to facilitate faster ER export (Saito et al., 2009). While these studies show that UPR activation by itself appears to modify the secretory pathway, that effect is different from the effects caused by luminal calcium depletion that are presented here.

The morphological changes that are observed in cells with luminal calcium depleted may impair the sorting efficiency in the ERGIC. While VSV-G transport to the Golgi and Golgi reformation were both strongly affected by calcium depletion, a bulk cargo marker was not (Figure 30). It is possibly that these seemingly conflicting results point to a specific defect in protein sorting in the ERGIC. In the ERGIC wayward ER proteins are packaged into COPI vesicles and returned to the ER (Figure 33). This results

in the concentration of proteins that are destined to a post-ERGIC compartment. A deficiency in the accurate sorting of anterograde cargo versus ER proteins could delay the maturation of intermediate compartment structures. Anterograde cargo that usually is excluded from retrograde vesicles may not be removed from these vesicles efficiently. This would cause the cargo to go through several rounds of trafficking. Delaying this maturation would result in an increased time during which the ERGIC accepts COPII vesicles that continue to bud from the ER. While ERGIC structures will still move away from the ERES at the same rate, only bulk flow cargo will maintain a constant transport rate. Any cargo that normally benefits from exclusion from retrograde vesicles will traffic slower. This would also result in an increase of VSV-G-GFP positive vesicles between the ERES and the ERGIC, as VSV-G-GFP would be sent back to the ER in COPI vesicles. Because normal light microscopy is resolution limited, it is possible that this accumulation of VSV-G-GFP vesicles could look structurally like the large accumulations of rbet1 and p24 that are observable during luminal calcium depletion.

The results presented here show that luminal calcium plays a regulatory role in the secretory pathway, but do not elucidate the precise mechanism. The chelation experiments show that, at least *in vitro*, it is likely that calcium leaking out of the vesicle is responsible for a decrease in membrane fusion. This conclusion implies the presence of calcium sensing machinery on the outside of the vesicle. A possible calcium sensor for this machinery is the penta-EF-hand protein Apoptosis Linked Gene 2 (ALG-2). ALG-2 has been implicated in stabilizing Sec31 at ERES in a calcium-dependent manner (Shibata et al., 2007; Yamasaki et al., 2006). Published results from the Hay laboratory show that ALG-2 is present on *in vitro* generated pre-Golgi intermediates (Bentley et al.,

2010). This interaction can be reversed by treatment with BAPTA. In addition to releasing ALG-2, COPII component attachment to ERGIC membranes is lost upon treatment with BAPTA. Conversely, treatment of intermediate structures with excess ALG-2 results in increased retention of COPII coat proteins. These experiments suggest that ALG-2 is a likely candidate to be the calcium sensor and that it plays a role in coat retention on the vesicle. It is possible that coat retention plays an important role in the sorting of cargo later in the secretory pathway. Retaining coat on the early ERGIC could be one way of maintaining micro domains that can be excluded from retrograde COPI vesicles. Any cargo that is not attached to the coat cannot be efficiently excluded from COPI buds, which results in return of the cargo molecule to the ER. This model also explains the seeming discrepancy between the VSV-G experiment and the *in vitro* results. While coat removal may result in faster homotypic vesicle fusion, the sorting steps required for ER to Golgi transport in intact cells produce the counterintuitive result of slower transport. Identifying the calcium sensor and its protein targets on the ERGIC membranes will provide insight into cargo sorting mechanisms that determine the fate of membrane cargoes.

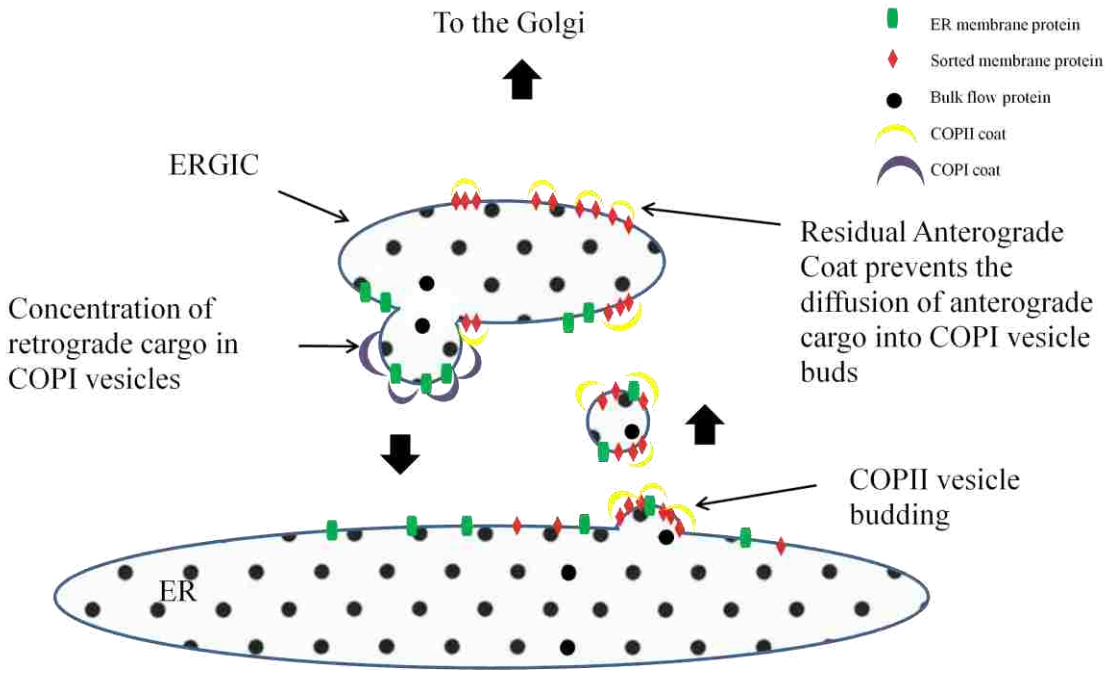

Figure 33 – A model for cargo sorting in the ERGIC.

Cargo is concentrated in COPII vesicles that bud from the ER. ERGIC structures receive COPII vesicles. ER proteins are concentrated in COPI vesicles that bud from the ERGIC while anterograde cargo is excluded from these vesicles. During and after this process the ERGIC structure is moved towards the Golgi apparatus.

References

Adler, E.M., G.J. Augustine, S.N. Duffy, and M.P. Charlton. 1991. Alien intracellular calcium chelators attenuate neurotransmitter release at the squid giant synapse. *J Neurosci*. 11:1496-507.

Aguilera-Romero, A., J. Kaminska, A. Spang, H. Riezman, and M. Muniz. 2008. The yeast p24 complex is required for the formation of COPI retrograde transport vesicles from the Golgi apparatus. *J Cell Biol*. 180:713-20.

Alberts, B., A. Johnson, J. Lewis, M. Raff, K. Roberts, and P. Walter. 2008. Molecular biology of the cell. Garland Science, New York. 1 v. (various pagings) pp.

Amodio, G., M. Renna, S. Paladino, C. Venturi, C. Tacchetti, O. Moltedo, S. Franceschelli, M. Mallardo, S. Bonatti, and P. Remondelli. 2009. Endoplasmic reticulum stress reduces the export from the ER and alters the architecture of post-ER compartments. *Int J Biochem Cell Biol*. 41:2511-21.

Appenzeller-Herzog, C., and H.P. Hauri. 2006. The ER-Golgi intermediate compartment (ERGIC): in search of its identity and function. *J Cell Sci*. 119:2173-83.

Argon, Y., and B.B. Simen. 1999. GRP94, an ER chaperone with protein and peptide binding properties. *Semin Cell Dev Biol*. 10:495-505.

Aridor, M., J. Weissman, S. Bannykh, C. Nuoffer, and W.E. Balch. 1998. Cargo selection by the COPII budding machinery during export from the ER. *J Cell Biol*. 141:61-70.

Barlowe, C., L. Orci, T. Yeung, M. Hosobuchi, S. Hamamoto, N. Salama, M.F. Rexach, M. Ravazzola, M. Amherdt, and R. Schekman. 1994. COPII: a membrane coat formed by Sec proteins that drive vesicle budding from the endoplasmic reticulum. *Cell*. 77:895-907.

Bassuk, J.A., and R.A. Berg. 1989. Protein disulphide isomerase, a multifunctional endoplasmic reticulum protein. *Matrix*. 9:244-58.

Beckers, C.J., and W.E. Balch. 1989. Calcium and GTP: essential components in vesicular trafficking between the endoplasmic reticulum and Golgi apparatus. *J Cell Biol*. 108:1245-56.

Belden, W.J., and C. Barlowe. 1996. Erv25p, a component of COPII-coated vesicles, forms a complex with Emp24p that is required for efficient endoplasmic reticulum to Golgi transport. *J Biol Chem*. 271:26939-46.

Bentley, M., Y. Liang, K. Mullen, D. Xu, E. Sztul, and J.C. Hay. 2006. SNARE status regulates tether recruitment and function in homotypic COPII vesicle fusion. *J Biol Chem*. 281:38825-33.

Bentley, M., D.C. Nycz, A. Joglekar, I. Fertschai, R. Malli, W.F. Graier, and J.C. Hay. 2010. Vesicular calcium regulates coat retention, fusogenicity, and size of pre-Golgi intermediates. *Mol Biol Cell*. 21:1033-46.

Bergmann, J.E. 1989. Using temperature-sensitive mutants of VSV to study membrane protein biogenesis. *Methods Cell Biol*. 32:85-110.

Bertolotti, A., Y. Zhang, L.M. Hendershot, H.P. Harding, and D. Ron. 2000. Dynamic interaction of BiP and ER stress transducers in the unfolded-protein response. *Nat Cell Biol*. 2:326-32.

Bhattacharyya, D., and B.S. Glick. 2007. Two mammalian Sec16 homologues have nonredundant functions in endoplasmic reticulum (ER) export and transitional ER organization. *Mol Biol Cell*. 18:839-49.

Bielli, A., C.J. Haney, G. Gabreski, S.C. Watkins, S.I. Bannykh, and M. Aridor. 2005. Regulation of Sar1 NH2 terminus by GTP binding and hydrolysis promotes membrane deformation to control COPII vesicle fission. *J Cell Biol*. 171:919-24.

Budnik, A., and D.J. Stephens. 2009. ER exit sites--localization and control of COPII vesicle formation. *FEBS Lett*. 583:3796-803.

Burgoyne, R.D., and M.J. Clague. 2003. Calcium and calmodulin in membrane fusion. *Biochim Biophys Acta*. 1641:137-43.

Bygrave, F.L., and A. Benedetti. 1996. What is the concentration of calcium ions in the endoplasmic reticulum? *Cell Calcium*. 19:547-51.

Cai, H., K. Reinisch, and S. Ferro-Novick. 2007a. Coats, tethers, Rabs, and SNAREs work together to mediate the intracellular destination of a transport vesicle. *Dev Cell*. 12:671-82.

Cai, H., S. Yu, S. Menon, Y. Cai, D. Lazarova, C. Fu, K. Reinisch, J.C. Hay, and S. Ferro-Novick. 2007b. TRAPPI tethers COPII vesicles by binding the coat subunit Sec23. *Nature*. 445:941-4.

Chao, D.S., J.C. Hay, S. Winnick, R. Prekeris, J. Klumperman, and R.H. Scheller. 1999. SNARE membrane trafficking dynamics in vivo. *J Cell Biol*. 144:869-81.

Chen, J.L., J.P. Ahluwalia, and M. Stamnes. 2002. Selective effects of calcium chelators on anterograde and retrograde protein transport in the cell. *J Biol Chem*. 277:35682-7.

Colombo, M.I., W. Beron, and P.D. Stahl. 1997. Calmodulin regulates endosome fusion. *J Biol Chem*. 272:7707-12.

Connerly, P.L., M. Esaki, E.A. Montegna, D.E. Strongin, S. Levi, J. Soderholm, and B.S. Glick. 2005. Sec16 is a determinant of transitional ER organization. *Curr Biol*. 15:1439-47.

Dancourt, J., and C. Barlowe. 2010. Protein sorting receptors in the early secretory pathway. *Annu Rev Biochem*. 79:777-802.

Dascher, C., J. Matteson, and W.E. Balch. 1994. Syntaxin 5 regulates endoplasmic reticulum to Golgi transport. *J Biol Chem*. 269:29363-6.

daSilva, L.L., E.L. Snapp, J. Denecke, J. Lippincott-Schwartz, C. Hawes, and F. Brandizzi. 2004. Endoplasmic reticulum export sites and Golgi bodies behave as single mobile secretory units in plant cells. *Plant Cell*. 16:1753-71.

de Silva, A., I. Braakman, and A. Helenius. 1993. Posttranslational folding of vesicular stomatitis virus G protein in the ER: involvement of noncovalent and covalent complexes. *J Cell Biol*. 120:647-55.

de Silva, A.M., W.E. Balch, and A. Helenius. 1990. Quality control in the endoplasmic reticulum: folding and misfolding of vesicular stomatitis virus G protein in cells and in vitro. *J Cell Biol*. 111:857-66.

Dirac-Svejstrup, A.B., T. Sumizawa, and S.R. Pfeffer. 1997. Identification of a GDI displacement factor that releases endosomal Rab GTPases from Rab-GDI. *EMBO J*. 16:465-72.

Dominguez, M., K. Dejgaard, J. Fullekrug, S. Dahan, A. Fazel, J.P. Paccaud, D.Y. Thomas, J.J. Bergeron, and T. Nilsson. 1998. gp25L/emp24/p24 protein family

members of the cis-Golgi network bind both COP I and II coatomer. *J Cell Biol*. 140:751-65.
Emery, G., M. Rojo, and J. Gruenberg. 2000. Coupled transport of p24 family members. *J Cell Sci*. 113 (Pt 13):2507-16.
Espenshade, P., R.E. Gimeno, E. Holzmacher, P. Teung, and C.A. Kaiser. 1995. Yeast SEC16 gene encodes a multidomain vesicle coat protein that interacts with Sec23p. *J Cell Biol*. 131:311-24.
Fath, S., J.D. Mancias, X. Bi, and J. Goldberg. 2007. Structure and organization of coat proteins in the COPII cage. *Cell*. 129:1325-36.
Foskett, J.K., C. White, K.H. Cheung, and D.O. Mak. 2007. Inositol trisphosphate receptor Ca2+ release channels. *Physiol Rev*. 87:593-658.
Fukuda, R., J.A. McNew, T. Weber, F. Parlati, T. Engel, W. Nickel, J.E. Rothman, and T.H. Sollner. 2000. Functional architecture of an intracellular membrane t-SNARE. *Nature*. 407:198-202.
Furst, J., R.B. Sutton, J. Chen, A.T. Brunger, and N. Grigorieff. 2003. Electron cryomicroscopy structure of N-ethyl maleimide sensitive factor at 11 A resolution. *EMBO J*. 22:4365-74.
Gething, M.J. 1999. Role and regulation of the ER chaperone BiP. *Semin Cell Dev Biol*. 10:465-72.
Gordon, D.E., L.M. Bond, D.A. Sahlender, and A.A. Peden. 2010. A targeted siRNA screen to identify SNAREs required for constitutive secretion in mammalian cells. *Traffic*. 11:1191-204.
Grosshans, B.L., D. Ortiz, and P. Novick. 2006. Rabs and their effectors: achieving specificity in membrane traffic. *Proc Natl Acad Sci U S A*. 103:11821-7.
Guy, J.E., E. Wigren, M. Svard, T. Hard, and Y. Lindqvist. 2008. New insights into multiple coagulation factor deficiency from the solution structure of human MCFD2. *J Mol Biol*. 381:941-55.
Harding, H.P., Y. Zhang, A. Bertolotti, H. Zeng, and D. Ron. 2000. Perk is essential for translational regulation and cell survival during the unfolded protein response. *Mol Cell*. 5:897-904.
Hay, J.C. 2007. Calcium: a fundamental regulator of intracellular membrane fusion? *EMBO Rep*. 8:236-40.
Hay, J.C., H. Hirling, and R.H. Scheller. 1996. Mammalian vesicle trafficking proteins of the endoplasmic reticulum and Golgi apparatus. *J Biol Chem*. 271:5671-9.
Hay, J.C., J. Klumperman, V. Oorschot, M. Steegmaier, C.S. Kuo, and R.H. Scheller. 1998. Localization, dynamics, and protein interactions reveal distinct roles for ER and Golgi SNAREs. *J Cell Biol*. 141:1489-502.
Haze, K., H. Yoshida, H. Yanagi, T. Yura, and K. Mori. 1999. Mammalian transcription factor ATF6 is synthesized as a transmembrane protein and activated by proteolysis in response to endoplasmic reticulum stress. *Mol Biol Cell*. 10:3787-99.
He, C.Y., M.K. Shaw, C.H. Pletcher, B. Striepen, L.G. Tilney, and D.S. Roos. 2001. A plastid segregation defect in the protozoan parasite Toxoplasma gondii. *EMBO J*. 20:330-9.
Hong, W. 2005. SNAREs and traffic. *Biochim Biophys Acta*. 1744:120-44.

Hughes, H., A. Budnik, K. Schmidt, K.J. Palmer, J. Mantell, C. Noakes, A. Johnson, D.A. Carter, P. Verkade, P. Watson, and D.J. Stephens. 2009. Organisation of human ER-exit sites: requirements for the localisation of Sec16 to transitional ER. *J Cell Sci*. 122:2924-34.

Hughes, H., and D.J. Stephens. 2008. Assembly, organization, and function of the COPII coat. *Histochem Cell Biol*. 129:129-51.

Iinuma, T., A. Shiga, K. Nakamoto, M.B. O'Brien, M. Aridor, N. Arimitsu, M. Tagaya, and K. Tani. 2007. Mammalian Sec16/p250 plays a role in membrane traffic from the endoplasmic reticulum. *J Biol Chem*. 282:17632-9.

Kirk, S.J., and T.H. Ward. 2007. COPII under the microscope. *Semin Cell Dev Biol*. 18:435-47.

Kreis, T.E., and H.F. Lodish. 1986. Oligomerization is essential for transport of vesicular stomatitis viral glycoprotein to the cell surface. *Cell*. 46:929-37.

Lee, M.C., L. Orci, S. Hamamoto, E. Futai, M. Ravazzola, and R. Schekman. 2005. Sar1p N-terminal helix initiates membrane curvature and completes the fission of a COPII vesicle. *Cell*. 122:605-17.

Levine, C.G., D. Mitra, A. Sharma, C.L. Smith, and R.S. Hegde. 2005. The efficiency of protein compartmentalization into the secretory pathway. *Mol Biol Cell*. 16:279-91.

Lippincott-Schwartz, J., L.C. Yuan, J.S. Bonifacino, and R.D. Klausner. 1989. Rapid redistribution of Golgi proteins into the ER in cells treated with brefeldin A: evidence for membrane cycling from Golgi to ER. *Cell*. 56:801-13.

Malhotra, J.D., and R.J. Kaufman. 2007. The endoplasmic reticulum and the unfolded protein response. *Semin Cell Dev Biol*. 18:716-31.

Malli, R., M. Frieden, M. Trenker, and W.F. Graier. 2005. The role of mitochondria for Ca2+ refilling of the endoplasmic reticulum. *J Biol Chem*. 280:12114-22.

Malli, R., S. Naghdi, C. Romanin, and W.F. Graier. 2008. Cytosolic Ca2+ prevents the subplasmalemmal clustering of STIM1: an intrinsic mechanism to avoid Ca2+ overload. *J Cell Sci*. 121:3133-9.

Malsam, J., S. Kreye, and T.H. Sollner. 2008. Membrane fusion: SNAREs and regulation. *Cell Mol Life Sci*. 65:2814-32.

Marz, K.E., J.M. Lauer, and P.I. Hanson. 2003. Defining the SNARE complex binding surface of alpha-SNAP: implications for SNARE complex disassembly. *J Biol Chem*. 278:27000-8.

Mason, M.J., C. Garcia-Rodriguez, and S. Grinstein. 1991. Coupling between intracellular Ca2+ stores and the Ca2+ permeability of the plasma membrane. Comparison of the effects of thapsigargin, 2,5-di-(tert-butyl)-1,4-hydroquinone, and cyclopiazonic acid in rat thymic lymphocytes. *J Biol Chem*. 266:20856-62.

Matsuoka, K., L. Orci, M. Amherdt, S.Y. Bednarek, S. Hamamoto, R. Schekman, and T. Yeung. 1998. COPII-coated vesicle formation reconstituted with purified coat proteins and chemically defined liposomes. *Cell*. 93:263-75.

Meldolesi, J., and T. Pozzan. 1998. The endoplasmic reticulum Ca2+ store: a view from the lumen. *Trends Biochem Sci*. 23:10-4.

Mezzacasa, A., and A. Helenius. 2002. The transitional ER defines a boundary for quality control in the secretion of tsO45 VSV glycoprotein. *Traffic*. 3:833-49.

Mironov, A.A., A.A. Mironov, Jr., G.V. Beznoussenko, A. Trucco, P. Lupetti, J.D. Smith, W.J. Geerts, A.J. Koster, K.N. Burger, M.E. Martone, T.J. Deerinck, M.H. Ellisman, and A. Luini. 2003. ER-to-Golgi carriers arise through direct en bloc protrusion and multistage maturation of specialized ER exit domains. *Dev Cell*. 5:583-94.

Miyawaki, A., J. Llopis, R. Heim, J.M. McCaffery, J.A. Adams, M. Ikura, and R.Y. Tsien. 1997. Fluorescent indicators for Ca2+ based on green fluorescent proteins and calmodulin. *Nature*. 388:882-7.

Montero, M., M. Brini, R. Marsault, J. Alvarez, R. Sitia, T. Pozzan, and R. Rizzuto. 1995. Monitoring dynamic changes in free Ca2+ concentration in the endoplasmic reticulum of intact cells. *EMBO J*. 14:5467-75.

Moussalli, M., S.W. Pipe, H.P. Hauri, W.C. Nichols, D. Ginsburg, and R.J. Kaufman. 1999. Mannose-dependent endoplasmic reticulum (ER)-Golgi intermediate compartment-53-mediated ER to Golgi trafficking of coagulation factors V and VIII. *J Biol Chem*. 274:32539-42.

Muniz, M., C. Nuoffer, H.P. Hauri, and H. Riezman. 2000. The Emp24 complex recruits a specific cargo molecule into endoplasmic reticulum-derived vesicles. *J Cell Biol*. 148:925-30.

Nagai, T., S. Yamada, T. Tominaga, M. Ichikawa, and A. Miyawaki. 2004. Expanded dynamic range of fluorescent indicators for Ca(2+) by circularly permuted yellow fluorescent proteins. *Proc Natl Acad Sci U S A*. 101:10554-9.

Nakano, A., D. Brada, and R. Schekman. 1988. A membrane glycoprotein, Sec12p, required for protein transport from the endoplasmic reticulum to the Golgi apparatus in yeast. *J Cell Biol*. 107:851-63.

Nebenfuhr, A., C. Ritzenthaler, and D.G. Robinson. 2002. Brefeldin A: deciphering an enigmatic inhibitor of secretion. *Plant Physiol*. 130:1102-8.

Nehls, S., E.L. Snapp, N.B. Cole, K.J. Zaal, A.K. Kenworthy, T.H. Roberts, J. Ellenberg, J.F. Presley, E. Siggia, and J. Lippincott-Schwartz. 2000. Dynamics and retention of misfolded proteins in native ER membranes. *Nat Cell Biol*. 2:288-95.

Novick, P., C. Field, and R. Schekman. 1980. Identification of 23 complementation groups required for post-translational events in the yeast secretory pathway. *Cell*. 21:205-15.

Nyfeler, B., B. Zhang, D. Ginsburg, R.J. Kaufman, and H.P. Hauri. 2006. Cargo selectivity of the ERGIC-53/MCFD2 transport receptor complex. *Traffic*. 7:1473-81.

Osibow, K., R. Malli, G.M. Kostner, and W.F. Graier. 2006. A new type of non-Ca2+-buffering Apo(a)-based fluorescent indicator for intraluminal Ca2+ in the endoplasmic reticulum. *J Biol Chem*. 281:5017-25.

Palmer, A.E., C. Jin, J.C. Reed, and R.Y. Tsien. 2004. Bcl-2-mediated alterations in endoplasmic reticulum Ca2+ analyzed with an improved genetically encoded fluorescent sensor. *Proc Natl Acad Sci U S A*. 101:17404-9.

Pepperkok, R., J. Scheel, H. Horstmann, H.P. Hauri, G. Griffiths, and T.E. Kreis. 1993. Beta-COP is essential for biosynthetic membrane transport from the endoplasmic reticulum to the Golgi complex in vivo. *Cell*. 74:71-82.

Peter, F., S.H. Wong, V.N. Subramaniam, B.L. Tang, and W. Hong. 1998. Alpha-SNAP but not gamma-SNAP is required for ER-Golgi transport after vesicle budding

and the Rab1-requiring step but before the EGTA-sensitive step. *J Cell Sci*. 111 (Pt 17):2625-33.
Peters, C., and A. Mayer. 1998. Ca2+/calmodulin signals the completion of docking and triggers a late step of vacuole fusion. *Nature*. 396:575-80.
Pezzati, R., M. Bossi, P. Podini, J. Meldolesi, and F. Grohovaz. 1997. High-resolution calcium mapping of the endoplasmic reticulum-Golgi-exocytic membrane system. Electron energy loss imaging analysis of quick frozen-freeze dried PC12 cells. *Mol Biol Cell*. 8:1501-12.
Porat, A., and Z. Elazar. 2000. Regulation of intra-Golgi membrane transport by calcium. *J Biol Chem*. 275:29233-7.
Presley, J.F., N.B. Cole, T.A. Schroer, K. Hirschberg, K.J. Zaal, and J. Lippincott-Schwartz. 1997. ER-to-Golgi transport visualized in living cells. *Nature*. 389:81-5.
Rivera, V.M., X. Wang, S. Wardwell, N.L. Courage, A. Volchuk, T. Keenan, D.A. Holt, M. Gilman, L. Orci, F. Cerasoli, Jr., J.E. Rothman, and T. Clackson. 2000. Regulation of protein secretion through controlled aggregation in the endoplasmic reticulum. *Science*. 287:826-30.
Rossanese, O.W., J. Soderholm, B.J. Bevis, I.B. Sears, J. O'Connor, E.K. Williamson, and B.S. Glick. 1999. Golgi structure correlates with transitional endoplasmic reticulum organization in Pichia pastoris and Saccharomyces cerevisiae. *J Cell Biol*. 145:69-81.
Ruddock, L.W., and M. Molinari. 2006. N-glycan processing in ER quality control. *J Cell Sci*. 119:4373-80.
Ruegsegger, U., J.H. Leber, and P. Walter. 2001. Block of HAC1 mRNA translation by long-range base pairing is released by cytoplasmic splicing upon induction of the unfolded protein response. *Cell*. 107:103-14.
Saito, A., S. Hino, T. Murakami, S. Kanemoto, S. Kondo, M. Saitoh, R. Nishimura, T. Yoneda, T. Furuichi, S. Ikegawa, M. Ikawa, M. Okabe, and K. Imaizumi. 2009. Regulation of endoplasmic reticulum stress response by a BBF2H7-mediated Sec23a pathway is essential for chondrogenesis. *Nat Cell Biol*. 11:1197-204.
Saraste, J., and K. Svensson. 1991. Distribution of the intermediate elements operating in ER to Golgi transport. *J Cell Sci*. 100 (Pt 3):415-30.
Schimmoller, F., B. Singer-Kruger, S. Schroder, U. Kruger, C. Barlowe, and H. Riezman. 1995. The absence of Emp24p, a component of ER-derived COPII-coated vesicles, causes a defect in transport of selected proteins to the Golgi. *EMBO J*. 14:1329-39.
Schroder, M. 2008. Endoplasmic reticulum stress responses. *Cell Mol Life Sci*. 65:862-94.
Shen, J., X. Chen, L. Hendershot, and R. Prywes. 2002. ER stress regulation of ATF6 localization by dissociation of BiP/GRP78 binding and unmasking of Golgi localization signals. *Dev Cell*. 3:99-111.
Shibata, H., H. Suzuki, H. Yoshida, and M. Maki. 2007. ALG-2 directly binds Sec31A and localizes at endoplasmic reticulum exit sites in a Ca2+-dependent manner. *Biochem Biophys Res Commun*. 353:756-63.

Sidrauski, C., and P. Walter. 1997. The transmembrane kinase Ire1p is a site-specific endonuclease that initiates mRNA splicing in the unfolded protein response. *Cell*. 90:1031-9.

Soldati, T., A.D. Shapiro, A.B. Svejstrup, and S.R. Pfeffer. 1994. Membrane targeting of the small GTPase Rab9 is accompanied by nucleotide exchange. *Nature*. 369:76-8.

Stamnes, M.A., M.W. Craighead, M.H. Hoe, N. Lampen, S. Geromanos, P. Tempst, and J.E. Rothman. 1995. An integral membrane component of coatomer-coated transport vesicles defines a family of proteins involved in budding. *Proc Natl Acad Sci U S A*. 92:8011-5.

Starai, V.J., N. Thorngren, R.A. Fratti, and W. Wickner. 2005. Ion regulation of homotypic vacuole fusion in Saccharomyces cerevisiae. *J Biol Chem*. 280:16754-62.

Strating, J.R., and G.J. Martens. 2009. The p24 family and selective transport processes at the ER-Golgi interface. *Biol Cell*. 101:495-509.

Strauss, J.H., and E.G. Strauss. 2008. Viruses and human disease. Elsevier / Academic Press, Amsterdam ; Boston. vii, 468 p. pp.

Supek, F., D.T. Madden, S. Hamamoto, L. Orci, and R. Schekman. 2002. Sec16p potentiates the action of COPII proteins to bud transport vesicles. *J Cell Biol*. 158:1029-38.

Sutton, R.B., D. Fasshauer, R. Jahn, and A.T. Brunger. 1998. Crystal structure of a SNARE complex involved in synaptic exocytosis at 2.4 A resolution. *Nature*. 395:347-53.

Taipale, M., D.F. Jarosz, and S. Lindquist. 2010. HSP90 at the hub of protein homeostasis: emerging mechanistic insights. *Nat Rev Mol Cell Biol*. 11:515-28.

Tang, B.L., D.Y. Low, and W. Hong. 1998. Hsec22c: a homolog of yeast Sec22p and mammalian rsec22a and msec22b/ERS-24. *Biochem Biophys Res Commun*. 243:885-91.

Tang, J., A. Maximov, O.H. Shin, H. Dai, J. Rizo, and T.C. Sudhof. 2006. A complexin/synaptotagmin 1 switch controls fast synaptic vesicle exocytosis. *Cell*. 126:1175-87.

Thor, F., M. Gautschi, R. Geiger, and A. Helenius. 2009. Bulk flow revisited: transport of a soluble protein in the secretory pathway. *Traffic*. 10:1819-30.

Trenker, M., R. Malli, I. Fertschai, S. Levak-Frank, and W.F. Graier. 2007. Uncoupling proteins 2 and 3 are fundamental for mitochondrial Ca2+ uniport. *Nat Cell Biol*. 9:445-52.

Ullrich, O., H. Horiuchi, C. Bucci, and M. Zerial. 1994. Membrane association of Rab5 mediated by GDP-dissociation inhibitor and accompanied by GDP/GTP exchange. *Nature*. 368:157-60.

Wagner, E.K., and M.J. Hewlett. 2004. Basic virology. Blackwell, Malden, MA. xxvi, 440 p. pp.

Watson, P., A.K. Townley, P. Koka, K.J. Palmer, and D.J. Stephens. 2006. Sec16 defines endoplasmic reticulum exit sites and is required for secretory cargo export in mammalian cells. *Traffic*. 7:1678-87.

Weber, T., B.V. Zemelman, J.A. McNew, B. Westermann, M. Gmachl, F. Parlati, T.H. Sollner, and J.E. Rothman. 1998. SNAREpins: minimal machinery for membrane fusion. *Cell*. 92:759-72.

Wieland, F.T., M.L. Gleason, T.A. Serafini, and J.E. Rothman. 1987. The rate of bulk flow from the endoplasmic reticulum to the cell surface. *Cell*. 50:289-300.

Williams, A.L., S. Ehm, N.C. Jacobson, D. Xu, and J.C. Hay. 2004. rsly1 binding to syntaxin 5 is required for endoplasmic reticulum-to-Golgi transport but does not promote SNARE motif accessibility. *Mol Biol Cell*. 15:162-75.

Wooding, S., and H.R. Pelham. 1998. The dynamics of golgi protein traffic visualized in living yeast cells. *Mol Biol Cell*. 9:2667-80.

Wuytack, F., L. Raeymaekers, and L. Missiaen. 2002. Molecular physiology of the SERCA and SPCA pumps. *Cell Calcium*. 32:279-305.

Xu, D., and J.C. Hay. 2004. Reconstitution of COPII vesicle fusion to generate a pre-Golgi intermediate compartment. *J Cell Biol*. 167:997-1003.

Yamasaki, A., K. Tani, A. Yamamoto, N. Kitamura, and M. Komada. 2006. The Ca2+-binding protein ALG-2 is recruited to endoplasmic reticulum exit sites by Sec31A and stabilizes the localization of Sec31A. *Mol Biol Cell*. 17:4876-87.

Yoshida, H., T. Okada, K. Haze, H. Yanagi, T. Yura, M. Negishi, and K. Mori. 2000. ATF6 activated by proteolysis binds in the presence of NF-Y (CBF) directly to the cis-acting element responsible for the mammalian unfolded protein response. *Mol Cell Biol*. 20:6755-67.

Zhang, B., R.J. Kaufman, and D. Ginsburg. 2005. LMAN1 and MCFD2 form a cargo receptor complex and interact with coagulation factor VIII in the early secretory pathway. *J Biol Chem*. 280:25881-6.

Zhang, B., B. McGee, J.S. Yamaoka, H. Guglielmone, K.A. Downes, S. Minoldo, G. Jarchum, F. Peyvandi, N.B. de Bosch, A. Ruiz-Saez, B. Chatelain, M. Olpinski, P. Bockenstedt, W. Sperl, R.J. Kaufman, W.C. Nichols, E.G. Tuddenham, and D. Ginsburg. 2006. Combined deficiency of factor V and factor VIII is due to mutations in either LMAN1 or MCFD2. *Blood*. 107:1903-7.

Zhang, Y.C., Y. Zhou, C.Z. Yang, and D.S. Xiong. 2009. A review of ERGIC-53: its structure, functions, regulation and relations with diseases. *Histol Histopathol*. 24:1193-204.